© 2014. Published by The Company of Biologists Ltd | Development (2014) 141, 1303-1312 doi:10.1242/dev.104513

RESEARCH ARTICLE

The putative PRC1 RING-finger protein AtRING1A regulates flowering through repressing *MADS AFFECTING FLOWERING* genes in *Arabidopsis*

Lisha Shen[1], Zhonghui Thong[1], Ximing Gong[1], Qing Shen[1], Yinbo Gan[2] and Hao Yu[1,*]

ABSTRACT

Polycomb group proteins play essential roles in the epigenetic control of gene expression in plants and animals. Although some components of Polycomb repressive complex 1 (PRC1)-like complexes have recently been reported in the model plant *Arabidopsis*, how they contribute to gene repression remains largely unknown. Here we show that a putative PRC1 RING-finger protein, AtRING1A, plays a hitherto unknown role in mediating the transition from vegetative to reproductive development in *Arabidopsis*. Loss of function of *AtRING1A* results in the late-flowering phenotype, which is attributed to derepression of two floral repressors, *MADS AFFECTING FLOWERING 4/5* (*MAF4*/*5*), which in turn downregulate two floral pathway integrators, *FLOWERING LOCUS T* and *SUPPRESSOR OF OVEREXPRESSION OF CONSTANS 1*. Levels of the H3K27me3 repressive mark at *MAF4* and *MAF5* loci, which is deposited by CURLY LEAF (CLF)-containing PRC2-like complexes and bound by LIKE HETEROCHROMATIN PROTEIN 1 (LHP1), are affected by AtRING1A, which interacts with both CLF and LHP1. Levels of the H3K4me3 activation mark correlate inversely with H3K27me3 levels at *MAF4* and *MAF5* loci. Our results suggest that AtRING1A suppresses the expression of *MAF4* and *MAF5* through affecting H3K27me3 levels at these loci to regulate the floral transition in *Arabidopsis*.

KEY WORDS: Polycomb repressive complex, Histone modification, Flowering time

INTRODUCTION

The transition from vegetative to reproductive growth, known as the floral transition, represents one of the most dramatic phase changes in flowering plants. In *Arabidopsis*, this process is regulated by a complex network of genetic pathways, including the photoperiod, vernalization, thermosensory, autonomous and gibberellin pathways (Amasino, 2010; Andrés and Coupland, 2012; Boss et al., 2004; Mouradov et al., 2002; Simpson and Dean, 2002; Srikanth and Schmid, 2011). *FLOWERING LOCUS C* (*FLC*) is a potent repressor of the flowering regulatory network that directly suppresses the expression of two floral pathway integrators, *FLOWERING LOCUS T* (*FT*) and *SUPPRESSOR OF OVEREXPRESSION OF CONSTANS 1* (*SOC1*) (Helliwell et al., 2006; Hepworth et al., 2002; Li et al., 2008; Michaels and Amasino, 1999; Searle et al., 2006; Sheldon et al., 2000). FRIGIDA (FRI) functions as a scaffold protein to interact with FRI-LIKE 1, FRI ESSENTIAL 1, SUPPRESSOR OF FRIGIDA 4 and FLC EXPRESSOR, and the resulting transcription activator complex (FRI-C) elevates *FLC* expression to inhibit flowering (Choi et al., 2011; Johanson et al., 2000; Michaels et al., 2004). By contrast, the vernalization and autonomous pathways repress *FLC* expression to promote flowering in response to prolonged cold exposure and developmental age, respectively (Michaels and Amasino, 2001; Sheldon et al., 2000). FLC and five close homologs, named MADS AFFECTING FLOWERING 1-5 (MAF1-5), belong to a small family of closely related MADS-box transcription factors (Parenicová et al., 2003). These *MAF* genes also repress the floral transition and their expression is influenced by vernalization (Gu et al., 2009; Kim and Sung, 2010; Ratcliffe et al., 2003; Ratcliffe et al., 2001; Sheldon et al., 2009; Sung et al., 2006).

Regulation of *FLC* and *MAF* genes involves extensive chromatin modifications at their loci (Amasino, 2004; He, 2009; He, 2012). For example, histone H3 lysine 4 (H3K4) trimethylation, H2B monoubiquitylation and H3K36 di- and trimethylation are associated with actively transcribed *FLC* chromatin, whereas repressive histone modifications, including histone deacetylation, H3K4 demethylation, H3K9 and H3K27 di- and trimethylation, and H4 arginine 3 symmetric dimethylation, are coupled with repression of *FLC*. In particular, the chromatin of *FLC*, *MAF4* and *MAF5* is associated with H3K27me3, which is a mark of transcriptionally silent chromatin (Alexandre and Hennig, 2008).

In *Drosophila*, in which Polycomb group (PcG) proteins were first identified, deposition of the repressive H3K27me3 mark is mediated by Polycomb repressive complex 2 (PRC2) (Schuettengruber et al., 2007). The PRC2 complex contains four core components: Enhancer of zeste [E(z)], Extra sex combs (Esc), Suppressor of zeste 12 [Su(z)12] and p55 (also known as Caf1 – FlyBase). PRC2 components are evolutionarily conserved in animals and plants. The homologs of PRC2 subunits have been identified in *Arabidopsis*, and have been shown to play crucial roles in regulating various developmental processes including the floral transition. For example, CURLY LEAF (CLF) is a homolog of E(z), the loss-of-function mutants of which flower precociously (Goodrich et al., 1997), and directly mediates the deposition of H3K27me3 at *FT*, *FLC*, *MAF4* and *MAF5*, thus repressing their mRNA expression (Jiang et al., 2008).

The PRC2 complex trimethylates H3K27. H3K27me3 is recognized and bound by the PRC1 complex that catalyzes the ubiquitylation of histone H2AK119, a mark for stabilizing the silenced state of H3K27me3-marked loci (Wang et al., 2004). The founding core PRC1 complex in *Drosophila* is composed of Polycomb (Pc), dRING1 [also known as Sex combs extra (Sce) – FlyBase], Posterior sex combs (Psc) and Polyhomeotic (Ph) (Francis et al., 2001; Shao et al., 1999), which have the corresponding

[1]Department of Biological Sciences and Temasek Life Sciences Laboratory, National University of Singapore, 10 Science Drive 4, 117543, Singapore. [2]Department of Agronomy, College of Agriculture and Biotechnology, Zhejiang University, Hangzhou 310058, China.

*Author for correspondence (dbsyuhao@nus.edu.sg)

Received 4 October 2013; Accepted 24 December 2013

Development (2014) doi:10.1242/dev.104513

mammalian homologs HPC, RING1A/B, BMI1 and HPH, respectively (Schwartz and Pirrotta, 2007). Unlike PRC2-like complexes, which have been extensively studied, the components of the PRC1-like complex were only recently identified in *Arabidopsis*. Although there is no homolog of Pc in *Arabidopsis*, a plant chromodomain protein, LIKE HETEROCHROMATIN PROTEIN 1 [LHP1; also known as TERMINAL FLOWER 2 (TFL2)], has been proposed to play a Pc-analogous function in binding H3K27me3 (Turck et al., 2007; Zhang et al., 2007). LHP1 regulates flowering time and is necessary for *FT* repression and maintaining vernalization-mediated *FLC* silencing after the plant resumes growth in warm conditions (Kotake et al., 2003; Mylne et al., 2006; Sung et al., 2006; Takada and Goto, 2003). Five PRC1 RING-finger proteins have been identified in the *Arabidopsis* genome (Sanchez-Pulido et al., 2008). AtRING1A and AtRING1B are homologous to RING1A/B, whereas AtBMI1A, AtBMI1B and AtBMI1C are homologous to BMI1. Investigations of mutants impaired in AtRING1A, AtRING1B, AtBMI1A, AtBMI1B and AtBMI1C have suggested that these PRC1 components are mainly involved in repressing embryonic and stem cell regulators (Bratzel et al., 2010; Chen et al., 2010; Xu and Shen, 2008; Yang et al., 2013). Although overexpression of *AtBMI1C* influences flowering time, downregulation of its expression does not show any defect (Li et al., 2011). In addition, *AtBMI1C* is an imprinted gene that is only expressed during endosperm and stamen development and in roots (Bratzel et al., 2012; Yang et al., 2013). Thus, *AtBMI1C* is unlikely to play an endogenous role in regulating flowering time.

Despite the progress in understanding PRC1 complexes in *Arabidopsis*, whether their different components regulate specific targets and how they interact with PRC2 to mediate gene repression are still largely unknown. It has recently been shown that LHP1 interacts with MULTICOPY SUPPRESSOR OF IRA1, a subunit of all PRC2 complexes in *Arabidopsis*, to facilitate the recruitment of PRC2 to target genes (Derkacheva et al., 2013). In this study, we report that AtRING1A plays a previously unidentified role in regulating the floral transition in *Arabidopsis*. We show that AtRING1A acts in conjunction with LHP1 and the key PRC2 component CLF to affect the levels of the H3K27me3 repressive mark at the *MAF4* and *MAF5* loci, thus repressing *MAF4* and *MAF5*, which in turn regulate two floral pathway integrators, *FT* and *SOC1*, to control flowering time in *Arabidopsis*.

RESULTS

Loss of function of *AtRING1A* shows late flowering

To study the role of PRC1 RING-finger proteins in plant development, we examined the phenotypes of the previously described mutant alleles of *AtRING1A*, *AtBMI1A* and *AtBMI1B* (Bratzel et al., 2010; Xu and Shen, 2008) and a novel T-DNA insertional mutant of *AtRING1B* obtained from the *Arabidopsis* Biological Resource Center, and found that only *Atring1a* (AL_945948) showed the obvious late-flowering phenotype under both long days (LDs) and short days (SDs) (Fig. 1A-D; supplementary material Fig. S1). As reported previously (Xu and Shen, 2008), *Atring1a* contained a T-DNA insertion at the end of the second intron (Fig. 1A) and did not produce *AtRING1A* transcripts spanning the T-DNA insertion site (Fig. 1B). To test whether the late-flowering phenotype of *Atring1a* is caused by loss of *AtRING1A* function, we transformed *Atring1a* mutants with a genomic construct (*gAtRING1A-4HA*) that contains a 5.4 kb *AtRING1A* genomic region including the 2.0 kb 5′ upstream sequence, the entire 3.0 kb coding sequence plus introns fused in frame with a 4HA tag, and the 0.4 kb 3′ untranslated region (UTR). For the majority of *Atring1a gAtRING1A-4HA* T1 transformants, flowering time was comparable to that of wild-type plants (Fig. 1E). This suggests that disruption of *AtRING1A* is responsible for the late-flowering phenotype of *Atring1a*.

In order to confirm the function of *AtRING1A* in flowering time regulation, we used artificial microRNA (AmiR) interference

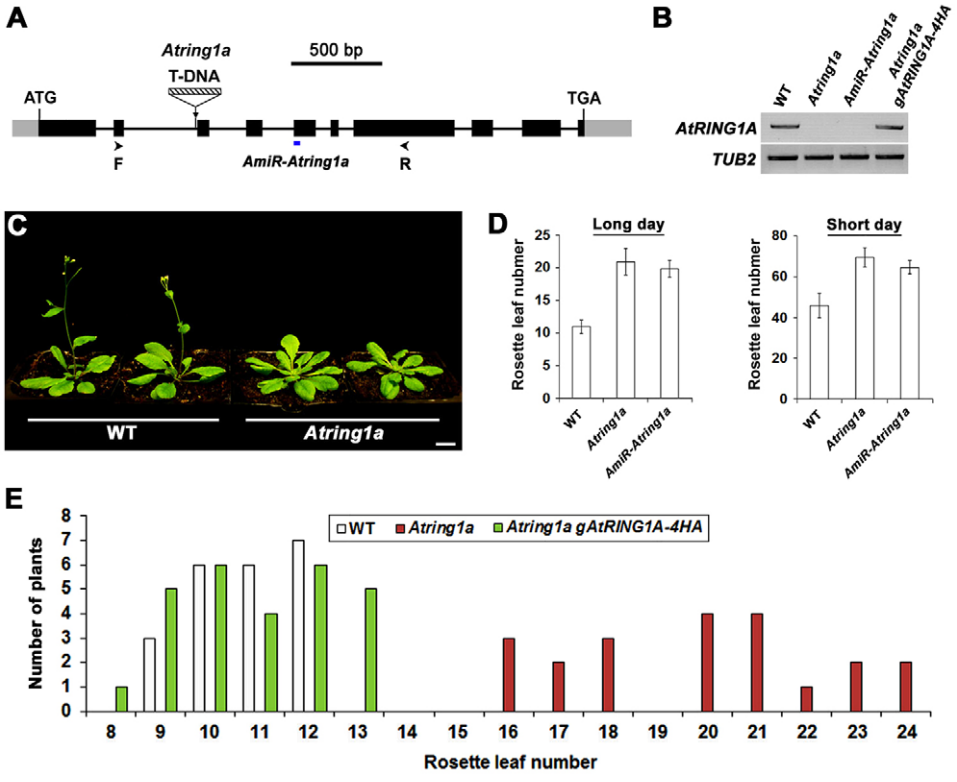

Fig. 1. *AtRING1A* regulates flowering time in *Arabidopsis*. (A) The T-DNA insertion in *Atring1a* (AL_945948) and the target site of the AmiR in *AmiR-Atring1a*. Exons and untranslated regions are represented by black and gray boxes, respectively, and introns are represented by black lines. Arrowheads indicate the positions of primers used for amplifying *AtRING1A* transcripts as shown in B. (B) RT-PCR showing that *AtRING1A* transcripts are not detectable in *Atring1a* and a representative *AmiR-Atring1a* line, but present in wild-type (WT) and *Atring1a gAtRING1A-4HA* plants. *TUB2* was amplified as a control. (C) *Atring1a* mutants show late flowering under LDs. Scale bar: 1 cm. (D) Flowering time of *Atring1a* and *AmiR-Atring1a* grown under LDs and SDs. Values were scored from at least 15 plants of each genotype. Error bars indicate s.d. (E) Distribution of flowering time in T1 transgenic lines carrying the *gAtRING1A-4HA* construct in an *Atring1a* background grown under LDs.

Development (2014) doi:10.1242/dev.104513

(Schwab et al., 2006) to knockdown *AtRING1A*, creating 18 independent *AmiR-Atring1a* lines that expressed an AmiR that specifically targeted *AtRING1A* exon 5 (Fig. 1A). Different levels of late flowering were displayed by 15 of these lines under LDs, and the line showing the latest flowering was chosen as a representative for further investigations. As expected, there were no detectable *AtRING1A* transcripts in this *AmiR-Atring1a* line that showed a comparable late-flowering phenotype to *Atring1a* mutants under both LDs and SDs (Fig. 1B,D), substantiating that *AtRING1A* functions in the promotion of flowering. We also created 25 transgenic plants overexpressing *AtRING1A*, all of which showed normal flowering time (data not shown), implying that overexpression of *AtRING1A* might not influence flowering.

Expression of *AtRING1A* during the floral transition

To examine the detailed tissue-specific expression pattern of *AtRING1A* during the floral transition, we generated a reporter construct with the genomic region of *AtRING1A* that was used for the complementation experiment (Fig. 1E), but without the 3′ UTR, fused to *GUS* (*gAtRING1A:GUS*). The staining patterns shown by most of the *gAtRING1A:GUS* transgenic plants were similar, and a representative line was chosen to further analyze *AtRING1A* expression during the floral transition. A 3-day-old *gAtRING1A:GUS* seedling showed specific GUS staining in the shoot apex and vascular tissues of cotyledons (Fig. 2A). In developing seedlings before, during and immediately after the floral transition occurring 9 to 13 days after germination under our growth conditions, GUS signals were consistently strong in shoot apices and vascular and mesophyll tissues of young leaves, but weak and finally absent in vascular tissues of older cotyledons or leaves (Fig. 2A; supplementary material Fig. S2). These patterns demonstrate that *AtRING1A* is highly expressed in actively proliferating cells during the floral transition.

Given that *AtRING1A* is involved in flowering time control, we further examined the effect of various flowering genetic pathways on *AtRING1A* expression during the floral transition. *AtRING1A* expression remained unchanged before and during the floral transition in wild-type plants grown under LDs (supplementary material Fig. S3A). Its expression was also unaffected in loss-of-function mutants of several key regulators in the photoperiod pathway (supplementary material Fig. S3B), suggesting that *AtRING1A* expression is not regulated by this pathway. *AtRING1A* was expressed at similar levels in GA-deficient *ga1-3* mutants and wild-type plants grown under SDs (supplementary material Fig. S4A). Consistently, GA treatment did not affect *AtRING1A* expression (supplementary material Fig. S4B), indicating that *AtRING1A* is not transcriptionally regulated by the GA pathway. Similarly, *AtRING1A* expression was unaffected in various mutants of the autonomous pathway (supplementary material Fig. S5A). Vernalization treatment did not affect *AtRING1A* expression, and *Atring1a* displayed a normal response to vernalization under both LDs and SDs (supplementary material Fig. S5B-D). These observations suggest that neither the autonomous pathway nor the vernalization pathway regulates *AtRING1A*. In addition, several other important flowering regulators, such as *SHORT VEGETATIVE PHASE* (*SVP*), *SOC1*, *AGAMOUS-LIKE 24* and *FLC*, which mediate flowering signals from various genetic pathways, did not affect *AtRING1A* expression (supplementary material Fig. S6). Taken together, these results suggest that *AtRING1A* is expressed in developing seedlings at fairly steady levels during the floral transition regardless of environmental and endogenous flowering signals, and that its mRNA expression is unaffected by floral pathway integrators, such as *SOC1* and *FT*.

AtRING1A promotes flowering through repressing *MAF4* and *MAF5*

Since AtRING1A is a PRC1 RING-finger protein that could affect the transcription of target genes, we proceeded to identify downstream targets of AtRING1A that might be responsible for its effects in promoting flowering. We examined the temporal expression of two floral pathways integrators, *SOC1* and *FT* (Blázquez and Weigel, 2000; Kardailsky et al., 1999; Kobayashi et al., 1999; Lee et al., 2000), and other known important flowering regulators, including *GIGANTEA* (*GI*), *CONSTANS* (*CO*), *AGL24*, *FLC*, *MAF* genes, *SVP*,

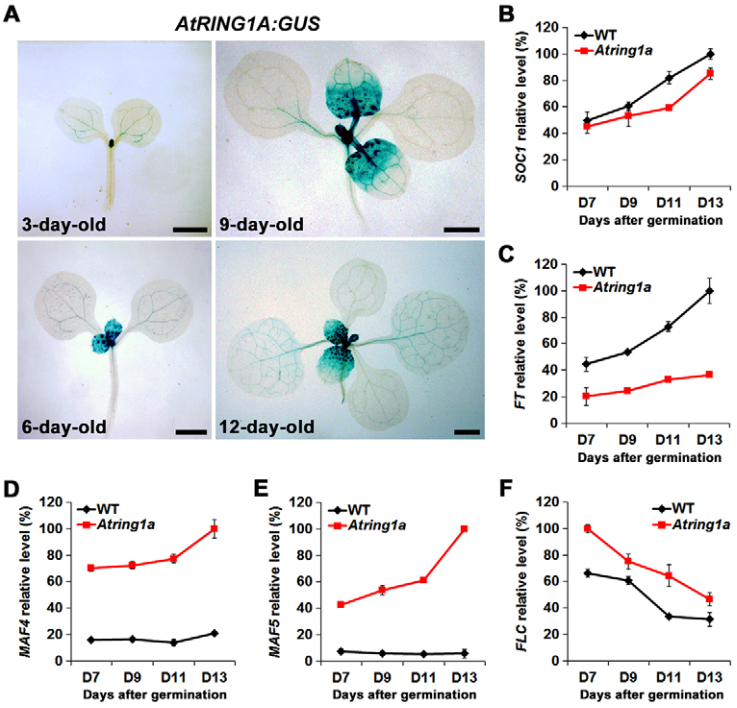

Fig. 2. Expression analysis of several key flowering time genes in *Atring1a* mutants during the floral transition. (A) GUS staining of developing *gAtRING1A:GUS* seedlings at the vegetative phase (3 and 6 days old) and during the floral transition (9 and 12 days old). Scale bars: 1 mm. (B-F) Temporal expression of *SOC1* (B), *FT* (C), *MAF4* (D), *MAF5* (E) and *FLC* (F) during the floral transition as determined by quantitative real-time PCR in developing wild-type and *Atring1a* seedlings grown under LDs. The levels of gene expression normalized to *TUB2* expression are shown relative to the maximal expression level set at 100%. Error bars indicate s.d.

Development (2014) doi:10.1242/dev.104513

TEMPRANILLO 1 (*TEM1*), *TEM2*, *SCHLAFMUTZE* (*SMZ*), *SCHNARCHZAPFEN* (*SNZ*), *TARGET OF EAT 1* (*TOE1*), *TOE2* and *TOE3* (Aukerman and Sakai, 2003; Castillejo and Pelaz, 2008; Hartmann et al., 2000; Li et al., 2008; Mathieu et al., 2009; Michaels and Amasino, 1999; Park et al., 1999; Putterill et al., 1995; Yant et al., 2010; Yu et al., 2002), in wild-type and *Atring1a* plants. Consistent with the late-flowering phenotype of *Atring1a*, both *FT* and *SOC1* were downregulated in developing *Atring1a* seedlings during the floral transition (Fig. 2B,C). It is noteworthy that, among all the floral repressors tested, only the expression of *MAF4* and *MAF5* was substantially upregulated in *Atring1a* mutants as compared with wild-type plants (Fig. 2D,E), whereas there was only a relatively moderate increase in *FLC* expression in *Atring1a* (Fig. 2F). The expression of the other *MAF* genes, *MAF1*, *MAF2* and *MAF3*, and of other flowering regulators was not obviously affected (supplementary material Fig. S7).

To study the regulatory hierarchy among *AtRING1A*, *MAF4*, *MAF5*, *FT* and *SOC1* during the floral transition, we analyzed the genetic interactions among these genes. We identified new mutant alleles of *MAF4* (*maf4-2*) and *MAF5* (*maf5-3*), each carrying a T-DNA insertion in their first intron (Fig. 3A), in which *MAF4* and *MAF5* cDNAs were not detectable (supplementary material Fig. S8). Consistent with previous studies (Gu et al., 2009; Kim and Sung, 2010), neither *maf4-2* nor *maf5-3* showed obvious flowering defects, but significantly rescued the late-flowering phenotype of *Atring1a* (Fig. 3B). These results demonstrate genetically that late flowering of *Atring1a* is mainly attributable to derepression of *MAF4* and *MAF5*. Overexpression of *SOC1* or *FT* greatly suppressed the late-flowering phenotype of *Atring1a*, whereas both *ft-10* and *soc1-2* enhanced the late-flowering phenotype (Fig. 3B). These observations, together with the expression analysis showing downregulation of *SOC1* and *FT* in *Atring1a* (Fig. 2B,C), indicate that *SOC1* and *FT* act downstream of *AtRING1A*.

To test whether *AtRING1A* promotes *FT* and *SOC1* expression through repressing *MAF4* and *MAF5*, we further compared the expression of *FT* and *SOC1* in 9-day-old *maf4-2 Atring1a* and *maf5-3 Atring1a* double mutants and their respective single mutants. Whereas *FT* and *SOC1* were downregulated in *Atring1a* as compared with wild-type seedlings, their expression in *maf4-2 Atring1a* and *maf5-3 Atring1a* was restored to levels close to those of wild-type seedlings (Fig. 3C). These expression data, together with the results of genetic crosses (Fig. 3B), strongly suggest that *AtRING1A* represses *MAF4* and *MAF5*, which in turn derepresses *FT* and *SOC1* to promote flowering.

AtRING1A affects H3K27me3 and H3K4me3 levels at *MAF4* and *MAF5*

Previous studies have suggested that histone modifications, such as H3K27me3 and H3K4me3, play important roles in regulating the expression of *MAF4* and *MAF5* (Jiang et al., 2011; Kim and Sung, 2010). As PRC1 subunits in animals and *Arabidopsis* have been shown to exert different effects on H3K27me3 at their target loci (Cao et al., 2005; Endoh et al., 2008; Wang et al., 2004; Yang et al., 2013), we examined whether AtRING1A, as a component of the PRC1 complexes, is involved in affecting H3K27me3 and H3K4me3 levels at *MAF4* and *MAF5*.

To test whether AtRING1A regulates the floral transition through affecting histone modifications, we first compared global methylation levels of H3K27 and H3K4 in 9-day-old *Atring1a* versus wild-type seedlings. There were no differences in mono-, di- or trimethylation levels at H3K4 and H3K27 in *Atring1a* and wild-type seedlings (supplementary material Fig. S9), indicating that AtRING1A does not affect the global methylation levels of H3K4 and H3K27 during the floral transition. We then measured H3K27me3 and H3K4me3 levels at the *MAF4* and *MAF5* loci by ChIP assays of 9-day-old wild-type and *Atring1a* seedlings. In wild-type seedlings, H3K27me3 was

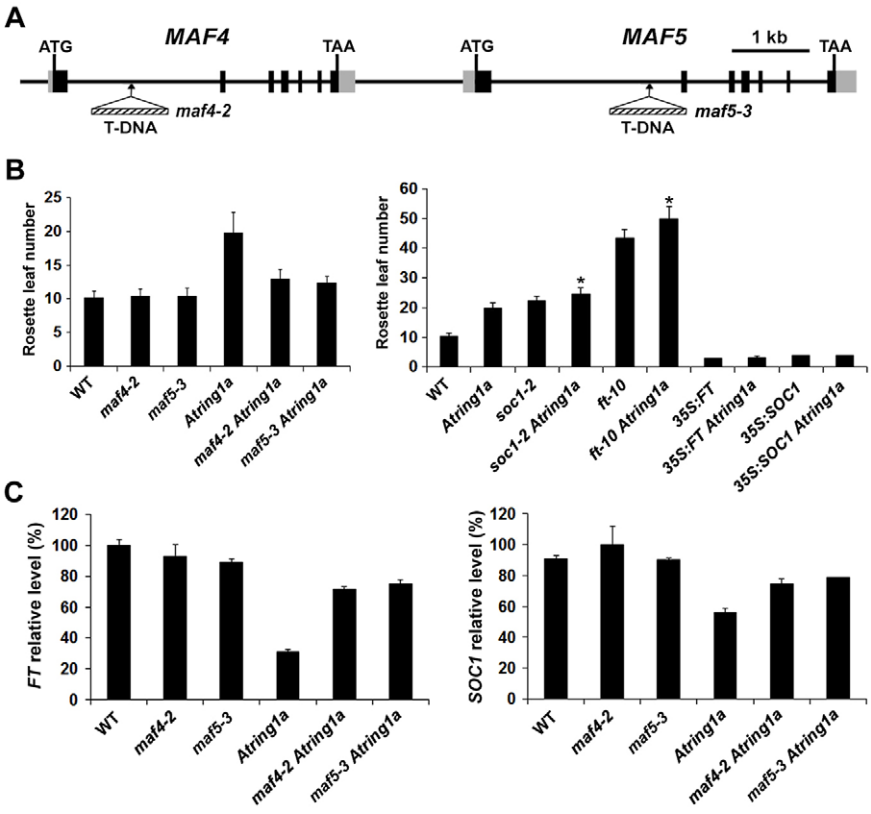

Fig. 3. Loss of function of *MAF4* or *MAF5* suppresses the late-flowering phenotype of *Atring1a*. (A) The T-DNA insertion in *maf4-2* (CS878527) and *maf5-3* (SALK_015513). Exons and untranslated regions are represented by black and gray boxes, respectively, and introns and other genomic regions are represented by black lines. Translation start sites (ATG) and stop codons (TAA) are indicated. (B) Flowering time of various mutants or transgenic plants grown under LDs. Values were scored from at least 15 plants of each genotype. **P*<0.05 (two-tailed paired Student's *t*-test) for flowering time of *soc1-2 Atring1a* and *ft-10 Atring1a* as compared with that of *Atring1a*. (C) Expression of *FT* and *SOC1* as determined by quantitative real-time PCR in 9-day-old seedlings of various mutants. The levels of gene expression normalized to *TUB2* expression are shown relative to the maximal expression level set at 100%. Error bars indicate s.d.

Development (2014) doi:10.1242/dev.104513

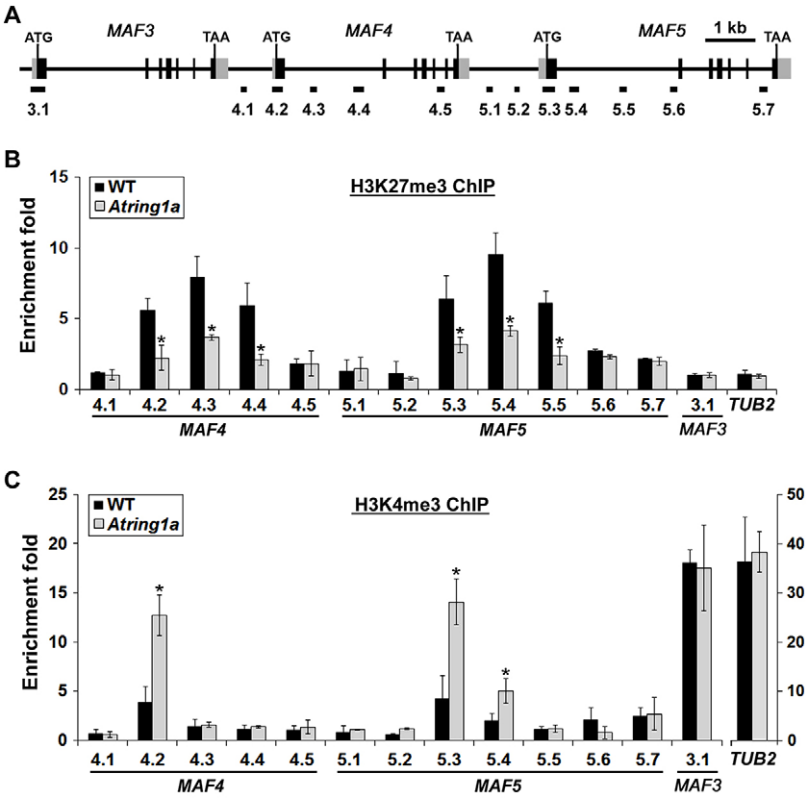

Fig. 4. *AtRING1A* affects H3K27me3 and H3K4me3 levels at *MAF4* and *MAF5*. (A) The genomic regions of *MAF3*, *MAF4* and *MAF5*. Exons and untranslated regions are represented by black and gray boxes, respectively, and introns and other genomic regions are represented by black lines. Translation start sites (ATG) and stop codons (TAA) are indicated. DNA fragments amplified in ChIP assays are indicated beneath the genomic regions. (B,C) ChIP analysis of H3K27me3 (B) and H3K4me3 (C) levels at *MAF4* and *MAF5* in 9-day-old wild-type and *Atring1a* seedlings. Genomic fragments of *MAF3* (3.1) and *TUB2* that are not targets of *AtRING1A* were amplified as negative controls. Error bars indicate s.d. of three biological replicates. **P*<0.05 (two-tailed paired Student's *t*-test) for ChIP fold enrichment between wild type and *Atring1a*.

clearly enriched in the genomic regions of *MAF4* and *MAF5* comprising the first exon and part of the following first intron, but not in the first exon of *MAF3* that is located immediately upstream of *MAF4* and *MAF5* (Fig. 4A,B). This observation is consistent with a previous study showing the enrichment of H3K27me3 at *MAF4* and *MAF5*, but not *MAF3* (Jiang et al., 2008). Notably, levels of H3K27me3 enrichment at *MAF4* and *MAF5* were generally reduced in *Atring1a* (Fig. 4A,B). Furthermore, H3K4me3 enrichment was detected around the transcription start sites of both *MAF4* and *MAF5* in wild-type seedlings, and the enrichment levels were strongly increased at these regions of *MAF4* and *MAF5* in *Atring1a* (Fig. 4A,C). In contrast to the change in H3K27me3 and H3K4me3 levels at *MAF4* and *MAF5*, both histone marks remained unchanged at *MAF3* and at a housekeeping gene, *TUB2*, in *Atring1a* versus wild-type seedlings (Fig. 4B,C).

The reciprocal changes in the levels of repressive H3K27me3 and permissive H3K4me3 marks at *MAF4* and *MAF5* correlated with upregulation of *MAF4* and *MAF5* in *Atring1a* (Fig. 2D,E). By contrast, H3K27me3 and H3K4me3 levels at *MAF3* and *FLC*, two close relatives of *MAF4* and *MAF5*, were not obviously altered in *Atring1a* (Fig. 4B,C; supplementary material Fig. S10), which is consistent with their unaltered and only slightly altered expression in *Atring1a*, respectively (Fig. 2F; supplementary material Fig. S7). These results suggest that AtRING1A is required for mediating H3K27me3 and H3K4me3 levels at the *MAF4* and *MAF5* loci to repress their transcription.

As a component of the PRC1 complex that catalyzes the ubiquitylation of histone H2AK119 (Wang et al., 2004), AtRING1A was shown to mediate H2A monoubiquitylation (H2Aub) *in vitro* (Bratzel et al., 2010). To test the endogenous effect of AtRING1A on H2AK119ub, we compared global H2AK119ub levels in 9-day-old *Atring1a* versus wild-type seedlings using a specific H2AK119ub antibody (Yang et al., 2013), and found that H2AK119ub levels were substantially increased in *Atring1a* compared with wild-type plants (supplementary material Fig. S11A). This could be due to increased H2AK119ub catalyzing activity of the other four PRC1 RING-finger proteins, namely AtRING1B, AtBMI1A, AtBMI1B and AtBMI1C, all of which were upregulated in mRNA expression in *Atring1a* (supplementary material Fig. S11B) (Chen et al., 2010). ChIP analysis further revealed that H2AK119ub was enriched at the transcriptional start sites of *MAF4* and *MAF5* in wild-type plants (supplementary material Fig. S11C). However, despite the change in global H2AK119ub levels in *Atring1a*, H2AK119ub levels at *MAF4* and *MAF5* were not significantly changed in *Atring1a* (supplementary material Fig. S11C), indicating that H2AK119ub might not directly contribute to the modulation of *MAF4* and *MAF5* expression by AtRING1A.

AtRING1A acts in conjunction with CLF and LHP1 to repress *MAF4* and *MAF5*

The observation that CLF, a component of PRC2-like complexes in *Arabidopsis*, is responsible for the deposition of H3K27me3 and the relevant change in H3K4me3 levels at *MAF4* and *MAF5* chromatin (Jiang et al., 2008) prompted us to investigate how AtRING1A and CLF, which have been shown to interact with each other *in vitro* and in yeast (Xu and Shen, 2008), act together to mediate H3K27me3 enrichment at *MAF4* and *MAF5* during the floral transition. We first measured H3K27me3 levels at *MAF4* and *MAF5* by ChIP assays of 9-day-old *Atring1a*, *clf* and *clf Atring1a* seedlings. As expected, H3K27me3 levels at *MAF4* and *MAF5* were strongly reduced in *clf* (Fig. 5A) (Jiang et al., 2008). In *clf Atring1a*, the enrichment of H3K27me3 at *MAF4* and *MAF5* was further reduced to levels lower than those in the respective single mutants (Fig. 5A). In agreement with the change in H3K27me3 levels at *MAF4* and *MAF5*, the expression of *MAF4* and *MAF5* was higher in *clf Atring1a* than in single mutants (Fig. 5B).

Development (2014) doi:10.1242/dev.104513

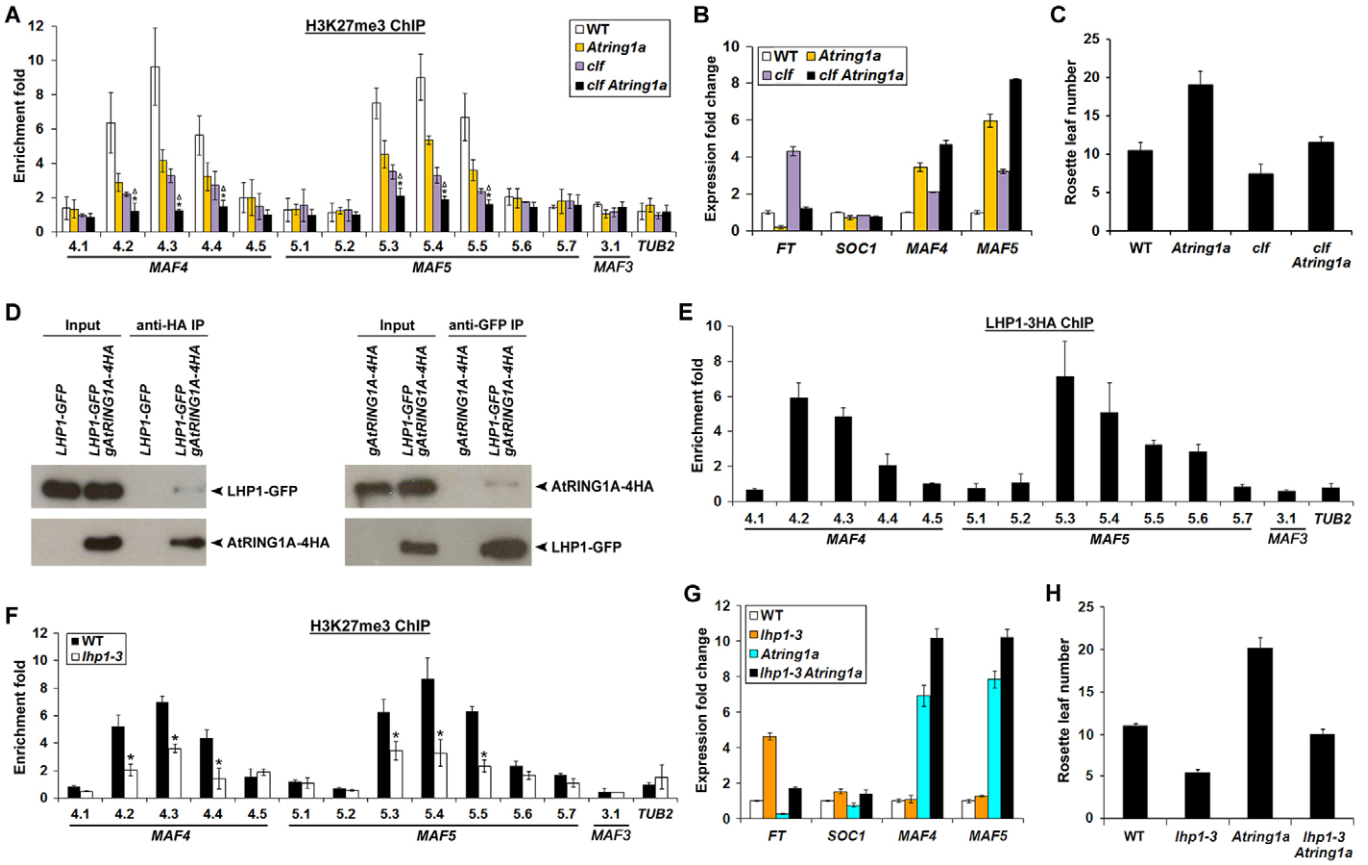

Fig. 5. AtRING1A acts in conjunction with CLF and LHP1 to repress *MAF4* and *MAF5* through affecting H3K27me3 levels at these two loci. (A) ChIP analysis of H3K27me3 levels at *MAF4* and *MAF5* in 9-day-old wild-type, *Atring1a*, *clf* and *clf Atring1a* seedlings. Genomic fragments of *MAF3* (3.1) and *TUB2* were amplified as negative controls. **P*<0.05 or $^{\Delta}P$<0.05 (two-tailed paired Student's *t*-test) for ChIP fold enrichment between *clf Atring1a* and *Atring1a* or between *clf Atring1a* and *clf*, respectively. (B) Quantitative real-time PCR analysis of expression of *FT*, *SOC1*, *MAF4* and *MAF5* in 9-day-old *Atring1a*, *clf* and *clf Atring1a* mutants grown under LDs. Results were normalized against the expression levels of *TUB2*. Gene expression levels in wild-type seedlings are all set as 1. (C) Flowering time of *Atring1a*, *clf* and *clf Atring1a* mutants grown under LDs. Values were scored from at least 15 plants of each genotype. (D) Reciprocal co-immunoprecipitation assays show that AtRING1A interacts with LHP1 *in vivo* during the floral transition. Nuclear extracts from 9-day-old *LHP1-GFP*, *gRING1A-4HA* and *LHP1-GFP gRING1A-4HA* plants were incubated with either anti-HA agarose or anti-GFP antibody bound to Protein G Plus-Agarose. The input and co-immunoprecipitated proteins were detected by anti-GFP (left upper and right lower panels) or anti-HA (left lower and right upper panels) antibody. (E) ChIP analysis of LHP1-3HA binding to the genomic regions of *MAF4* and *MAF5*. Nine-day-old *lhp1-3 35S:LHP1-3HA* plants were harvested for ChIP analysis. Genomic fragments of *MAF3* (3.1) and *TUB2* were amplified as negative controls. Fold enrichment of each fragment was calculated first by normalizing the amount of a target DNA fragment against a genomic fragment of *ACTIN7* (*At5g09810*) as an internal control, and then by normalizing the value for *lhp1-3 35S:LHP1-3HA* against that for *lhp1-3* plants. (F) Loss of *LHP1* results in reduced H3K27me3 levels at *MAF4* and *MAF5* loci. ChIP analysis of H3K27me3 levels at *MAF4* and *MAF5* was performed on 9-day-old wild-type and *lhp1-3* seedlings. **P*<0.05 (two-tailed paired Student's *t*-test) for ChIP fold enrichment between *lhp1-3* and wild-type plants. (G) Quantitative real-time PCR analysis of expression of *FT*, *SOC1*, *MAF4* and *MAF5* in 9-day-old *lhp1-3*, *Atring1a* and *lhp1-3 Atring1a* mutants grown under LDs. Results were normalized against the expression levels of *TUB2*. Gene expression levels in wild-type seedlings are all set as 1. (H) Flowering time of *lhp1-3*, *Atring1a* and *lhp1-3 Atring1a* mutants grown under LDs. Values were scored from at least 15 plants of each genotype. Error bars indicate s.d.

As CLF-dependent H3K27me3 suppresses the expression of many flowering promoters and repressors (Jiang et al., 2008; Schönrock et al., 2006), loss of *CLF* function in *clf* simultaneously derepresses these genes, including the potent flowering promoter *FT*, resulting in an early-flowering phenotype (Fig. 5B,C) (Jiang et al., 2008; Schönrock et al., 2006). *clf Atring1a* double mutants exhibited later flowering than *clf* single mutants, demonstrating that *Atring1a* partially suppresses early flowering of *clf* (Fig. 5C). This observation is in line with the finding that two floral repressors, *MAF4* and *MAF5*, are more substantially derepressed in *clf Atring1a* than in *clf* (Fig. 5B). Taken together, these results strongly suggest that AtRING1A acts in conjunction with CLF to repress *MAF4* and *MAF5* through affecting H3K27me3 levels at these two loci to regulate flowering time.

Although ChIP analysis of *Atring1a gAtRING1A-4HA* transgenic lines (Fig. 1E) did not reveal direct binding of AtRING1A to *MAF4* and *MAF5* genomic regions (supplementary material Fig. S12), AtRING1A has been suggested to interact with another putative PRC1 component, LHP1 (Bratzel et al., 2010; Chen et al., 2010; Xu and Shen, 2008), which may have a Pc-analogous function in binding H3K27me3-marked genomic regions (Turck et al., 2007; Zhang et al., 2007). Indeed, we detected *in vivo* interaction between AtRING1A-4HA and LHP1-GFP (Kotake et al., 2003) during the floral transition (Fig. 5D). Consistent with previous data from genome-wide analysis of LHP1 binding (Turck et al., 2007; Zhang et al., 2007), ChIP analysis using 9-day-old *lhp1-3 35S:LHP1-3HA* seedlings (Liu et al., 2009) showed that LHP1-3HA was bound to the genomic regions marked with H3K27me3 at *MAF4* and *MAF5*

Development (2014) doi:10.1242/dev.104513

(Fig. 4B, Fig. 5E). H3K27me3 levels at *MAF4* and *MAF5* were also reduced in *lhp1-3* (Fig. 5F), which is in line with a recent study showing that LHP1 is required for establishing full H3K27me3 levels of PcG target genes (Derkacheva et al., 2013). These results indicate that AtRING1A interacts with LHP1 to affect H3K27me3 levels at *MAF4* and *MAF5*. Surprisingly, *MAF4* and *MAF5* expression was not obviously altered in *lhp1-3* as compared with wild-type plants (Fig. 5G). This might be attributable to the effect of *LHP1* on multiple flowering genes (Kotake et al., 2003; Sung et al., 2006) that may directly or indirectly affect *MAF4* and *MAF5* expression. However, *MAF4* and *MAF5* were more derepressed in *lhp1-3 Atring1a* than in *Atring1a* (Fig. 5G), showing a synergistic effect of AtRING1A and LHP1 on the expression of *MAF4* and *MAF5*. As a result, *Atring1a* partially suppressed early flowering of *lhp1-3* (Fig. 5H). These observations, together with the similar expression patterns of *AtRING1A* and *LHP1* in actively proliferating cells (Fig. 2A) (Kotake et al., 2003), indicate that AtRING1A and LHP1 could act in the same PRC1-like complexes to repress *MAF4* and *MAF5* during the floral transition.

DISCUSSION

The PRC1 RING-finger proteins AtRING1A, AtRING1B, AtBMI1A, AtBMI1B and AtBMI1C were recently identified in the model plant *Arabidopsis*, and studies on these proteins have so far been focused on their function in regulating a few common targets involved in the repression of embryonic traits and meristem maintenance at the vegetative phase (Bratzel et al., 2010; Chen et al., 2010; Xu and Shen, 2008; Yang et al., 2013). Although AtBMI1A and AtBMI1B have been shown to mediate H2A monoubiquitylation and ubiquitin-dependent proteasomal degradation of a targeted transcription factor in *Arabidopsis* (Bratzel et al., 2010; Qin et al., 2008), how these PRC1 subunits contribute to gene silencing during plant development is still largely unknown. In this study, we report that AtRING1A acts as an important regulator of flowering in *Arabidopsis*, revealing a hitherto unknown role of a PRC1 RING-finger protein in mediating the transition from vegetative to reproductive development in plants. Loss of function of *AtRING1A* significantly delays flowering, which is due to derepression of *MAF4* and *MAF5* and the resulting downregulation of two floral pathway integrators, *FT* and *SOC1*.

The floral transition regulated by AtRING1A is a key developmental process that is simultaneously regulated by PRC2-like complexes in *Arabidopsis*. This provides a unique paradigm for studying the relationship between PRC1-like and PRC2-like complexes in plants. Enrichment of the H3K27me3 repressive mark at *MAF4* and *MAF5* loci, which is deposited by the CLF-containing PRC2-like complexes, is also affected by AtRING1A, which interacts with CLF. The expression levels of *MAF4* and *MAF5* consistently correlate with the changes in H3K27me3 levels at these two loci in *Atring1a*, *clf* and *clf Atring1a* (Fig. 5A,B). These findings suggest that the AtRING1A-containing PRC1-like complexes could act in conjunction with the CLF-containing PRC2 complexes to suppress the expression of *MAF4* and *MAF5* through affecting their H3K27me3 levels to regulate the floral transition in *Arabidopsis* (Fig. 6).

Interestingly, AtRING1A and CLF show additive rather than redundant effects on H3K27me3 enrichment at *MAF4* and *MAF5* (Fig. 5A), indicating that both proteins are required for this methylation. In the canonical model of PRC1 action, PRC2 deposits the H3K27me3 mark that sequentially recruits PRC1, which then catalyzes the ubiquitylation of H2AK119 to maintain the silenced state of H3K27me3-marked loci (Cao et al., 2005; Wang et al., 2004). This hierarchical model explains why the knockout of some PRC1 subunits in animals and plants does not affect the upstream event of H3K27me3 enrichment deposited by PRC2 at their target genes (Bratzel et al., 2010; Cao et al., 2005; Chen et al., 2010; Wang et al., 2004; Xu and Shen, 2008). However, this model of chromatin modification is challenged by the decrease in H3K27me3 levels observed at target genes in RING1A/B-deficient embryonic stem cells (Endoh et al., 2008). A recent study has shown that AtBMI1A, AtBMI1B and AtBMI1C are required for the H3K27me3 modification of seed maturation genes in *Arabidopsis* (Yang et al., 2013). Similarly, the impact of AtRING1A on H3K27me3 enrichment at *MAF4* and *MAF5* revealed in our study also implies that the concerted action of PRC1 and PRC2 could at least include their cooperative effect in mediating H3K27me3 levels at some of their common target genes.

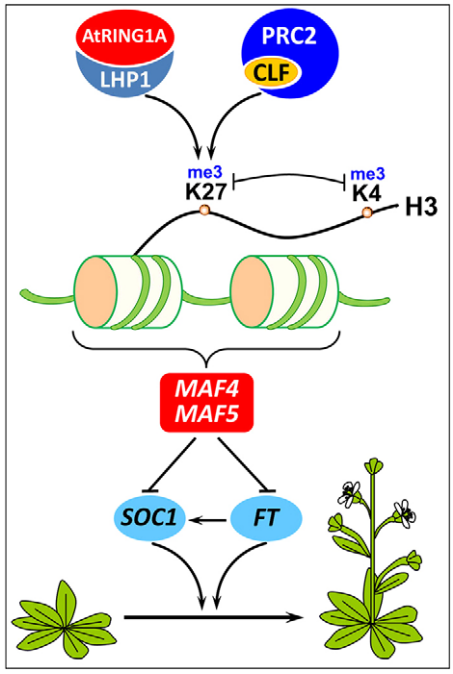

Fig. 6. Model of AtRING1A function in mediating the floral transition. The PRC1 RING-finger protein AtRING1A regulates the floral transition by suppressing the expression of two flowering repressors, *MAF4* and *MAF5*, which in turn upregulates two floral pathway integrators, *FT* and *SOC1*, and promotes flowering. Levels of the H3K27me3 repressive mark at *MAF4* and *MAF5* loci, which is deposited by the CLF-containing PRC2-like complexes and bound by LHP1, are affected by AtRING1A, which interacts with both CLF and LHP1. Alteration of H3K4me3 levels correlates inversely with H3K27me3 levels at *MAF4* and *MAF5* loci. Promotive interactions are indicated by arrows and repressive interactions are indicated by T-bars.

The function of AtRING1A in mediating H3K27me3 levels could be restricted to a limited number of target genes in a specific developmental context. As shown in this study, although AtRING1A affects H3K27me3 levels at *MAF4* and *MAF5*, global H3K27 methylation levels are not altered in *Atring1a* as compared with wild-type plants during the floral transition, indicating that AtRING1A might only affect H3K27me3 levels at a few specific flowering regulators. This is in contrast to the functional mode of CLF, a histone methyltransferase in PRC2-like complexes, the knockout mutants of which show a reduction in global H3K27me3 levels during the floral transition (Jiang et al., 2008). In line with the contribution of CLF and AtRING1A to global H3K27me3 levels,

Development (2014) doi:10.1242/dev.104513

CLF represses the expression of a group of flowering time genes including important flowering promoters and repressors, such as *FLC*, *MAF4*, *MAF5* and *FT* (Jiang et al., 2008; Schönrock et al., 2006), whereas AtRING1A only specifically represses the two flowering repressors *MAF4* and *MAF5* but not the other repressors tested, including their close relatives *MAF1-3* and *FLC*. The difference in the target specificity of AtRING1A and CLF might in part correlate with the status of their physical interaction with target genes. CLF has been shown to directly bind to the chromatin of its target genes, such as *FLC*, *MAF4*, *MAF5* and *FT* (Jiang et al., 2008). By contrast, the interaction between AtRING1A and the chromatin of *MAF4* and *MAF5* seems to be mediated by other regulators, potentially including LHP1, which is largely associated with H3K27me3-marked loci (Turck et al., 2007; Zhang et al., 2007). As none of the plant PRC1 RING-finger proteins has so far been reported to bind to their target genes, how their interacting partners contribute to targeting specificity of PRC1 RING-finger proteins is an intriguing question that remains to be investigated further.

The mammalian PRC1 RING-finger proteins form an E3 ubiquitin ligase complex that catalyzes histone H2AK119 ubiquitylation (H2AK119ub) (Cao et al., 2005; de Napoles et al., 2004; Wang et al., 2004). Although it has been suggested that H2AK119ub could play a role in blocking transcription elongation by restraining RNA polymerase movement through the compacted nucleosomes (Simon and Kingston, 2009), the precise underlying mechanism for PRC1-mediated gene repression is still largely unknown. All five *Arabidopsis* PRC1 RING-finger proteins, including AtRING1A, have also been shown to mediate H2Aub *in vivo* or *in vitro* (Bratzel et al., 2010; Bratzel et al., 2012; Li et al., 2011). However, AtRING1A is the only RING-finger protein with knockout mutants that exhibit the flowering phenotype, which is due to the elevated expression of *MAF4* and *MAF5*. In addition, AtRING1A does not affect H2AK119ub levels at *MAF4* and *MAF5*. These results imply that the effect of AtRING1A on the expression of *MAF4* and *MAF5* and on H3K27me3 levels at these two loci is at least independent of PRC1-mediated H2AK119ub during the floral transition. This example, together with other studies showing the independence of H2AK119ub and PRC1-mediated gene repression (Eskeland et al., 2010; Richly et al., 2010; Yang et al., 2013), indicate that the regulation and outcome of PRC1 activity are far more complex than previously thought.

In summary, the PRC1 RING-finger protein AtRING1A acts together with the key PRC2 component CLF to suppress the expression of two flowering repressors, *MAF4* and *MAF5*, through affecting H3K27me3 levels at these two loci. This previously unidentified similarity in the pattern of PRC1 and PRC2 action on specific target genes in plants demonstrates the functional complexity of PcG proteins in generating chromatin-modifying complexes that target specific genes in a given developmental context.

MATERIALS AND METHODS

Plant materials and growth conditions

Arabidopsis thaliana plants were grown on soil or Murashige and Skoog (MS) medium under LDs (16 hours light/8 hours dark) or SDs (8 hours light/16 hours dark). The mutants *co-1*, *gi-1*, *ft-10*, *fve-3*, *soc1-2*, *agl24-1*, *svp-41*, *maf4-2*, *maf5-3*, *clf*, *Atring1a*, *Atring1b-2*, *Atbmi1a-1* and *Atbmi1b* are in the Columbia (Col) background, whereas *co-2*, *fca-1*, *fpa-1*, *fve-1* and *ga1-3* are in the Landsberg *erecta* (L*er*) background (Bratzel et al., 2010; Li et al., 2008; Shen et al., 2011; Xu and Shen, 2008). *Atring1a* (AL_945948), *Atring1b-2* (SALK_143481C), *Atbmi1a-1* (SALK_145041), *Atbmi1b* (CS855837), *maf4-2* (CS878527), *maf5-3* (SALK_015513) and *clf* (SALK_006658) seeds were obtained from the *Arabidopsis* Biological Resource Center (http://www.arabidopsis.org/). All transgenic plants were generated through *Agrobacterium tumefaciens*-mediated transformation. Transformants harboring *gAtRING1A-4HA* were selected on MS medium supplemented with kanamycin, whereas those harboring *gAtRING1A:GUS* were selected by Basta on soil.

Plasmid construction

To construct *gAtRING1A-4HA*, a 5.4 kb *AtRING1A* genomic fragment (*gAtRING1A*) was amplified using primers gAtRING1A-F and gAtRING1A-R and cloned into pENTR/D-TOPO (Invitrogen). Based on this construct, gAtRING1A-4HA was generated using a modified QuikChange site-directed mutagenesis approach (Geiser et al., 2001). The sequence encoding 4HA was amplified with primers gAtRING1A-4HA-F and gAtRING1A-4HA-R, and the resulting PCR products were then annealed to the methylated *gAtRING1A* plasmid and elongated with Phusion Hot Start II High-Fidelity DNA polymerase (Finnzymes). After *Dpn*I digestion, the mutated plasmids containing the 4HA fragment were recovered from *E. coli* transformants. To construct *gAtRING1A:GUS* (*β-glucuronidase*), a 5.0 kb *AtRING1A* genomic fragment was amplified with primers gAtRING1A-F (*Eco*RI) and gAtRING1A-R (*Bam*HI) and cloned into pHY107 (Liu et al., 2007). The primers used for plasmid construction are listed in supplementary material Table S1.

Expression analysis

Total RNA was extracted using the FavorPrep Plant Total RNA Mini Kit (Favorgen) and reverse transcribed using M-MLV reverse transcriptase (Promega). Quantitative real-time PCR was performed in triplicate on each of three independently collected samples using the 7900HT Fast Real-Time PCR System (Applied Biosystems) with Maxima SYBR Green/ROX qPCR Master Mix (Fermentas). The expression of *TUBULIN 2* (*TUB2*) was used as an internal control. Relative expression levels of genes were calculated as previously described (Liu et al., 2007). The primers used for real-time PCR are listed in supplementary material Table S1.

GUS staining

GUS staining of *gAtRING1A:GUS* transgenic plants was carried out as previously described (Tao et al., 2012; Yu et al., 2000). Seedlings were first fixed in ice-cold 90% acetone for 20 minutes. After three washes in rinse solution [50 mM Na_2HPO_4, 50 mM NaH_2PO_4, 0.5 mM $K_3Fe(CN)_6$, 0.5 mM $K_4Fe(CN)_6$], the seedlings were infiltrated with staining solution (rinse solution with 2 mM X-Gluc) under vacuum and subsequently incubated at 37°C for 6 hours. The stained tissues were cleared of chlorophyll in an ethanol series and observed under a light microscope.

Chromatin immunoprecipitation (ChIP) assay

ChIP assay was performed as previously described (Shen et al., 2011). Seedlings were fixed on ice in MC buffer (10 mM potassium phosphate pH 7.0, 50 mM NaCl, 0.1 M sucrose) with 1% formaldehyde under vacuum for 45 minutes, after which the fixed seedlings were homogenized in liquid nitrogen. The chromatin was extracted and sonicated to produce DNA fragments of ~500 bp. H3K27me3 and H3K4me3 were detected by anti-H3K27me3 and anti-H3K4me3 antibodies (Upstate Biotechnology) bound to Protein A/G Plus-Agarose (Santa Cruz). Fold-enrichment of each fragment was determined by quantitative real-time PCR as previously described (Li et al., 2008). Genomic fragments of *ACTIN7* (*At5g09810*) and *MU* (*At4g03870*) were amplified as internal controls for measurement of H3K27me3 and H3K4me3 enrichment, respectively. ChIP assays were repeated with at least three biological replicates. Unless stated otherwise, fold enrichment of each fragment was calculated first by normalizing the amount of a target DNA fragment against a genomic fragment of an internal control, and then by normalizing the value for immunoprecipitated samples against that for input. Primer pairs used for ChIP assays are listed in supplementary material Table S1.

Co-immunoprecipitation

Nine-day-old seedlings were ground with a mortar and pestle in liquid nitrogen and nuclear proteins were extracted. The protein extracts were then incubated overnight with anti-HA agarose conjugate (Sigma) or anti-GFP

antibody (Invitrogen) bound to Protein G Plus-Agarose (Santa Cruz) at 4°C. The immunoprecipitated proteins and the protein extracts as inputs were resolved by SDS-PAGE and detected by anti-HA (Santa Cruz) or anti-GFP antibody (Santa Cruz).

Western blot analysis

Nuclear proteins were extracted from plant materials according to the ChIP protocol, but without the tissue fixation step. Proteins were resolved by SDS-PAGE and detected using various histone antibodies, including those detecting H3K4me1, H3K4me2, H3K4me3, H3K27me1, H3K27me2, H3k27me3, H3 (Upstate Biotechnology) and H2AK119ub (Cell Signaling).

Acknowledgements

We thank Dr Koji Goto for kindly providing the seeds of *LHP1-GFP*, Dr Lu Liu for critical reading of the manuscript, and the *Arabidopsis* Biological Resource Center for providing seeds of *Atring1a*, *Atring1b-2*, *Atbmi1a-1*, *Atbmi1b*, *maf4-2*, *maf5-3* and *clf*.

Competing interests

The authors declare no competing financial interests.

Author contributions

L.S. and H.Y. conceived and designed the experiments; L.S., Z.T., X.G. and Q.S. performed the experiments; L.S., Y.G. and H.Y. analyzed the data; L.S. and H.Y. wrote the manuscript.

Funding

This work was supported by Academic Research Funds [MOE2011-T2-1-018 and MOE2011-T2-2-008] from the Ministry of Education, Singapore; the National Natural Science Foundation of China [grant no. 31228002]; and intramural resource support from the National University of Singapore and Temasek Life Sciences Laboratory.

Supplementary material

Supplementary material available online at
http://dev.biologists.org/lookup/suppl/doi:10.1242/dev.104513/-/DC1

References

Alexandre, C. M. and Hennig, L. (2008). FLC or not FLC: the other side of vernalization. *J. Exp. Bot.* **59**, 1127-1135.
Amasino, R. (2004). Vernalization, competence, and the epigenetic memory of winter. *Plant Cell* **16**, 2553-2559.
Amasino, R. (2010). Seasonal and developmental timing of flowering. *Plant J.* **61**, 1001-1013.
Andrés, F. and Coupland, G. (2012). The genetic basis of flowering responses to seasonal cues. *Nat. Rev. Genet.* **13**, 627-639.
Aukerman, M. J. and Sakai, H. (2003). Regulation of flowering time and floral organ identity by a MicroRNA and its APETALA2-like target genes. *Plant Cell* **15**, 2730-2741.
Blázquez, M. A. and Weigel, D. (2000). Integration of floral inductive signals in Arabidopsis. *Nature* **404**, 889-892.
Boss, P. K., Bastow, R. M., Mylne, J. S. and Dean, C. (2004). Multiple pathways in the decision to flower: enabling, promoting, and resetting. *Plant Cell* **16 Suppl. 1**, S18-S31.
Bratzel, F., López-Torrejón, G., Koch, M., Del Pozo, J. C. and Calonje, M. (2010). Keeping cell identity in Arabidopsis requires PRC1 RING-finger homologs that catalyze H2A monoubiquitination. *Curr. Biol.* **20**, 1853-1859.
Bratzel, F., Yang, C., Angelova, A., López-Torrejón, G., Koch, M., del Pozo, J. C. and Calonje, M. (2012). Regulation of the new Arabidopsis imprinted gene AtBMI1C requires the interplay of different epigenetic mechanisms. *Mol. Plant* **5**, 260-269.
Cao, R., Tsukada, Y. and Zhang, Y. (2005). Role of Bmi-1 and Ring1A in H2A ubiquitylation and Hox gene silencing. *Mol. Cell* **20**, 845-854.
Castillejo, C. and Pelaz, S. (2008). The balance between CONSTANS and TEMPRANILLO activities determines FT expression to trigger flowering. *Curr. Biol.* **18**, 1338-1343.
Chen, D., Molitor, A., Liu, C. and Shen, W. H. (2010). The Arabidopsis PRC1-like ring-finger proteins are necessary for repression of embryonic traits during vegetative growth. *Cell Res.* **20**, 1332-1344.
Choi, K., Kim, J., Hwang, H. J., Kim, S., Park, C., Kim, S. Y. and Lee, I. (2011). The FRIGIDA complex activates transcription of FLC, a strong flowering repressor in Arabidopsis, by recruiting chromatin modification factors. *Plant Cell* **23**, 289-303.
de Napoles, M., Mermoud, J. E., Wakao, R., Tang, Y. A., Endoh, M., Appanah, R., Nesterova, T. B., Silva, J., Otte, A. P., Vidal, M. et al. (2004). Polycomb group proteins Ring1A/B link ubiquitylation of histone H2A to heritable gene silencing and X inactivation. *Dev. Cell* **7**, 663-676.
Derkacheva, M., Steinbach, Y., Wildhaber, T., Mozgová, I., Mahrez, W., Nanni, P., Bischof, S., Gruissem, W. and Hennig, L. (2013). Arabidopsis MSI1 connects LHP1 to PRC2 complexes. *EMBO J.* **32**, 2073-2085.
Endoh, M., Endo, T. A., Endoh, T., Fujimura, Y., Ohara, O., Toyoda, T., Otte, A. P., Okano, M., Brockdorff, N., Vidal, M. et al. (2008). Polycomb group proteins Ring1A/B are functionally linked to the core transcriptional regulatory circuitry to maintain ES cell identity. *Development* **135**, 1513-1524.
Eskeland, R., Leeb, M., Grimes, G. R., Kress, C., Boyle, S., Sproul, D., Gilbert, N., Fan, Y., Skoultchi, A. I., Wutz, A. et al. (2010). Ring1B compacts chromatin structure and represses gene expression independent of histone ubiquitination. *Mol. Cell* **38**, 452-464.
Francis, N. J., Saurin, A. J., Shao, Z. and Kingston, R. E. (2001). Reconstitution of a functional core polycomb repressive complex. *Mol. Cell* **8**, 545-556.
Geiser, M., Cèbe, R., Drewello, D. and Schmitz, R. (2001). Integration of PCR fragments at any specific site within cloning vectors without the use of restriction enzymes and DNA ligase. *Biotechniques* **31**, 88-90, 92.
Goodrich, J., Puangsomlee, P., Martin, M., Long, D., Meyerowitz, E. M. and Coupland, G. (1997). A Polycomb-group gene regulates homeotic gene expression in Arabidopsis. *Nature* **386**, 44-51.
Gu, X., Jiang, D., Wang, Y., Bachmair, A. and He, Y. (2009). Repression of the floral transition via histone H2B monoubiquitination. *Plant J.* **57**, 522-533.
Hartmann, U., Höhmann, S., Nettesheim, K., Wisman, E., Saedler, H. and Huijser, P. (2000). Molecular cloning of SVP: a negative regulator of the floral transition in Arabidopsis. *Plant J.* **21**, 351-360.
He, Y. (2009). Control of the transition to flowering by chromatin modifications. *Mol. Plant* **2**, 554-564.
He, Y. (2012). Chromatin regulation of flowering. *Trends Plant Sci.* **17**, 556-562.
Helliwell, C. A., Wood, C. C., Robertson, M., James Peacock, W. and Dennis, E. S. (2006). The Arabidopsis FLC protein interacts directly in vivo with SOC1 and FT chromatin and is part of a high-molecular-weight protein complex. *Plant J.* **46**, 183-192.
Hepworth, S. R., Valverde, F., Ravenscroft, D., Mouradov, A. and Coupland, G. (2002). Antagonistic regulation of flowering-time gene SOC1 by CONSTANS and FLC via separate promoter motifs. *EMBO J.* **21**, 4327-4337.
Jiang, D., Wang, Y., Wang, Y. and He, Y. (2008). Repression of FLOWERING LOCUS C and FLOWERING LOCUS T by the Arabidopsis Polycomb repressive complex 2 components. *PLoS ONE* **3**, e3404.
Jiang, D., Kong, N. C., Gu, X., Li, Z. and He, Y. (2011). Arabidopsis COMPASS-like complexes mediate histone H3 lysine-4 trimethylation to control floral transition and plant development. *PLoS Genet.* **7**, e1001330.
Johanson, U., West, J., Lister, C., Michaels, S., Amasino, R. and Dean, C. (2000). Molecular analysis of FRIGIDA, a major determinant of natural variation in Arabidopsis flowering time. *Science* **290**, 344-347.
Kardailsky, I., Shukla, V. K., Ahn, J. H., Dagenais, N., Christensen, S. K., Nguyen, J. T., Chory, J., Harrison, M. J. and Weigel, D. (1999). Activation tagging of the floral inducer FT. *Science* **286**, 1962-1965.
Kim, D. H. and Sung, S. (2010). The plant homeo domain finger protein, VIN3-LIKE 2, is necessary for photoperiod-mediated epigenetic regulation of the floral repressor, MAF5. *Proc. Natl. Acad. Sci. USA* **107**, 17029-17034.
Kobayashi, Y., Kaya, H., Goto, K., Iwabuchi, M. and Araki, T. (1999). A pair of related genes with antagonistic roles in mediating flowering signals. *Science* **286**, 1960-1962.
Kotake, T., Takada, S., Nakahigashi, K., Ohto, M. and Goto, K. (2003). Arabidopsis TERMINAL FLOWER 2 gene encodes a heterochromatin protein 1 homolog and represses both FLOWERING LOCUS T to regulate flowering time and several floral homeotic genes. *Plant Cell Physiol.* **44**, 555-564.
Lee, H., Suh, S. S., Park, E., Cho, E., Ahn, J. H., Kim, S. G., Lee, J. S., Kwon, Y. M. and Lee, I. (2000). The AGAMOUS-LIKE 20 MADS domain protein integrates floral inductive pathways in Arabidopsis. *Genes Dev.* **14**, 2366-2376.
Li, D., Liu, C., Shen, L., Wu, Y., Chen, H., Robertson, M., Helliwell, C. A., Ito, T., Meyerowitz, E. and Yu, H. (2008). A repressor complex governs the integration of flowering signals in Arabidopsis. *Dev. Cell* **15**, 110-120.
Li, W., Wang, Z., Li, J., Yang, H., Cui, S., Wang, X. and Ma, L. (2011). Overexpression of AtBMI1C, a polycomb group protein gene, accelerates flowering in Arabidopsis. *PLoS ONE* **6**, e21364.
Liu, C., Zhou, J., Bracha-Drori, K., Yalovsky, S., Ito, T. and Yu, H. (2007). Specification of Arabidopsis floral meristem identity by repression of flowering time genes. *Development* **134**, 1901-1910.
Liu, C., Xi, W., Shen, L., Tan, C. and Yu, H. (2009). Regulation of floral patterning by flowering time genes. *Dev. Cell* **16**, 711-722.
Mathieu, J., Yant, L. J., Mürdter, F., Küttner, F. and Schmid, M. (2009). Repression of flowering by the miR172 target SMZ. *PLoS Biol.* **7**, e1000148.
Michaels, S. D. and Amasino, R. M. (1999). FLOWERING LOCUS C encodes a novel MADS domain protein that acts as a repressor of flowering. *Plant Cell* **11**, 949-956.
Michaels, S. D. and Amasino, R. M. (2001). Loss of FLOWERING LOCUS C activity eliminates the late-flowering phenotype of FRIGIDA and autonomous pathway mutations but not responsiveness to vernalization. *Plant Cell* **13**, 935-941.
Michaels, S. D., Bezerra, I. C. and Amasino, R. M. (2004). FRIGIDA-related genes are required for the winter-annual habit in Arabidopsis. *Proc. Natl. Acad. Sci. USA* **101**, 3281-3285.
Mouradov, A., Cremer, F. and Coupland, G. (2002). Control of flowering time: interacting pathways as a basis for diversity. *Plant Cell* **14 Suppl.**, S111-S130.
Mylne, J. S., Barrett, L., Tessadori, F., Mesnage, S., Johnson, L., Bernatavichute, Y. V., Jacobsen, S. E., Fransz, P. and Dean, C. (2006). LHP1, the Arabidopsis homologue of HETEROCHROMATIN PROTEIN1, is required for epigenetic silencing of FLC. *Proc. Natl. Acad. Sci. USA* **103**, 5012-5017.

Parenicová, L., de Folter, S., Kieffer, M., Horner, D. S., Favalli, C., Busscher, J., Cook, H. E., Ingram, R. M., Kater, M. M., Davies, B. et al. (2003). Molecular and phylogenetic analyses of the complete MADS-box transcription factor family in Arabidopsis: new openings to the MADS world. *Plant Cell* **15**, 1538-1551.

Park, D. H., Somers, D. E., Kim, Y. S., Choy, Y. H., Lim, H. K., Soh, M. S., Kim, H. J., Kay, S. A. and Nam, H. G. (1999). Control of circadian rhythms and photoperiodic flowering by the Arabidopsis GIGANTEA gene. *Science* **285**, 1579-1582.

Putterill, J., Robson, F., Lee, K., Simon, R. and Coupland, G. (1995). The CONSTANS gene of Arabidopsis promotes flowering and encodes a protein showing similarities to zinc finger transcription factors. *Cell* **80**, 847-857.

Qin, F., Sakuma, Y., Tran, L. S., Maruyama, K., Kidokoro, S., Fujita, Y., Fujita, M., Umezawa, T., Sawano, Y., Miyazono, K. et al. (2008). Arabidopsis DREB2A-interacting proteins function as RING E3 ligases and negatively regulate plant drought stress-responsive gene expression. *Plant Cell* **20**, 1693-1707.

Ratcliffe, O. J., Nadzan, G. C., Reuber, T. L. and Riechmann, J. L. (2001). Regulation of flowering in Arabidopsis by an FLC homologue. *Plant Physiol.* **126**, 122-132.

Ratcliffe, O. J., Kumimoto, R. W., Wong, B. J. and Riechmann, J. L. (2003). Analysis of the Arabidopsis MADS AFFECTING FLOWERING gene family: MAF2 prevents vernalization by short periods of cold. *Plant Cell* **15**, 1159-1169.

Richly, H., Rocha-Viegas, L., Ribeiro, J. D., Demajo, S., Gundem, G., Lopez-Bigas, N., Nakagawa, T., Rospert, S., Ito, T. and Di Croce, L. (2010). Transcriptional activation of polycomb-repressed genes by ZRF1. *Nature* **468**, 1124-1128.

Sanchez-Pulido, L., Devos, D., Sung, Z. R. and Calonje, M. (2008). RAWUL: a new ubiquitin-like domain in PRC1 ring finger proteins that unveils putative plant and worm PRC1 orthologs. *BMC Genomics* **9**, 308.

Schönrock, N., Bouveret, R., Leroy, O., Borghi, L., Köhler, C., Gruissem, W. and Hennig, L. (2006). Polycomb-group proteins repress the floral activator AGL19 in the FLC-independent vernalization pathway. *Genes Dev.* **20**, 1667-1678.

Schuettengruber, B., Chourrout, D., Vervoort, M., Leblanc, B. and Cavalli, G. (2007). Genome regulation by polycomb and trithorax proteins. *Cell* **128**, 735-745.

Schwab, R., Ossowski, S., Riester, M., Warthmann, N. and Weigel, D. (2006). Highly specific gene silencing by artificial microRNAs in Arabidopsis. *Plant Cell* **18**, 1121-1133.

Schwartz, Y. B. and Pirrotta, V. (2007). Polycomb silencing mechanisms and the management of genomic programmes. *Nat. Rev. Genet.* **8**, 9-22.

Searle, I., He, Y., Turck, F., Vincent, C., Fornara, F., Kröber, S., Amasino, R. A. and Coupland, G. (2006). The transcription factor FLC confers a flowering response to vernalization by repressing meristem competence and systemic signaling in Arabidopsis. *Genes Dev.* **20**, 898-912.

Shao, Z., Raible, F., Mollaaghababa, R., Guyon, J. R., Wu, C. T., Bender, W. and Kingston, R. E. (1999). Stabilization of chromatin structure by PRC1, a Polycomb complex. *Cell* **98**, 37-46.

Sheldon, C. C., Rouse, D. T., Finnegan, E. J., Peacock, W. J. and Dennis, E. S. (2000). The molecular basis of vernalization: the central role of FLOWERING LOCUS C (FLC). *Proc. Natl. Acad. Sci. USA* **97**, 3753-3758.

Sheldon, C. C., Finnegan, E. J., Peacock, W. J. and Dennis, E. S. (2009). Mechanisms of gene repression by vernalization in Arabidopsis. *Plant J.* **59**, 488-498.

Shen, L., Kang, Y. G., Liu, L. and Yu, H. (2011). The J-domain protein J3 mediates the integration of flowering signals in Arabidopsis. *Plant Cell* **23**, 499-514.

Simon, J. A. and Kingston, R. E. (2009). Mechanisms of polycomb gene silencing: knowns and unknowns. *Nat. Rev. Mol. Cell Biol.* **10**, 697-708.

Simpson, G. G. and Dean, C. (2002). Arabidopsis, the Rosetta stone of flowering time? *Science* **296**, 285-289.

Srikanth, A. and Schmid, M. (2011). Regulation of flowering time: all roads lead to Rome. *Cell. Mol. Life Sci.* **68**, 2013-2037.

Sung, S., He, Y., Eshoo, T. W., Tamada, Y., Johnson, L., Nakahigashi, K., Goto, K., Jacobsen, S. E. and Amasino, R. M. (2006). Epigenetic maintenance of the vernalized state in Arabidopsis thaliana requires LIKE HETEROCHROMATIN PROTEIN 1. *Nat. Genet.* **38**, 706-710.

Takada, S. and Goto, K. (2003). Terminal flower2, an Arabidopsis homolog of heterochromatin protein1, counteracts the activation of flowering locus T by constans in the vascular tissues of leaves to regulate flowering time. *Plant Cell* **15**, 2856-2865.

Tao, Z., Shen, L., Liu, C., Liu, L., Yan, Y. and Yu, H. (2012). Genome-wide identification of SOC1 and SVP targets during the floral transition in Arabidopsis. *Plant J.* **70**, 549-561.

Turck, F., Roudier, F., Farrona, S., Martin-Magniette, M. L., Guillaume, E., Buisine, N., Gagnot, S., Martienssen, R. A., Coupland, G. and Colot, V. (2007). Arabidopsis TFL2/LHP1 specifically associates with genes marked by trimethylation of histone H3 lysine 27. *PLoS Genet.* **3**, e86.

Wang, H., Wang, L., Erdjument-Bromage, H., Vidal, M., Tempst, P., Jones, R. S. and Zhang, Y. (2004). Role of histone H2A ubiquitination in Polycomb silencing. *Nature* **431**, 873-878.

Xu, L. and Shen, W. H. (2008). Polycomb silencing of KNOX genes confines shoot stem cell niches in Arabidopsis. *Curr. Biol.* **18**, 1966-1971.

Yang, C., Bratzel, F., Hohmann, N., Koch, M., Turck, F. and Calonje, M. (2013). VAL- and AtBMI1-mediated H2Aub initiate the switch from embryonic to postgerminative growth in Arabidopsis. *Curr. Biol.* **23**, 1324-1329.

Yant, L., Mathieu, J., Dinh, T. T., Ott, F., Lanz, C., Wollmann, H., Chen, X. and Schmid, M. (2010). Orchestration of the floral transition and floral development in Arabidopsis by the bifunctional transcription factor APETALA2. *Plant Cell* **22**, 2156-2170.

Yu, H., Yang, S. H. and Goh, C. J. (2000). DOH1, a class 1 knox gene, is required for maintenance of the basic plant architecture and floral transition in orchid. *Plant Cell* **12**, 2143-2160.

Yu, H., Xu, Y., Tan, E. L. and Kumar, P. P. (2002). AGAMOUS-LIKE 24, a dosage-dependent mediator of the flowering signals. *Proc. Natl. Acad. Sci. USA* **99**, 16336-16341.

Zhang, X., Germann, S., Blus, B. J., Khorasanizadeh, S., Gaudin, V. and Jacobsen, S. E. (2007). The Arabidopsis LHP1 protein colocalizes with histone H3 Lys27 trimethylation. *Nat. Struct. Mol. Biol.* **14**, 869-871.

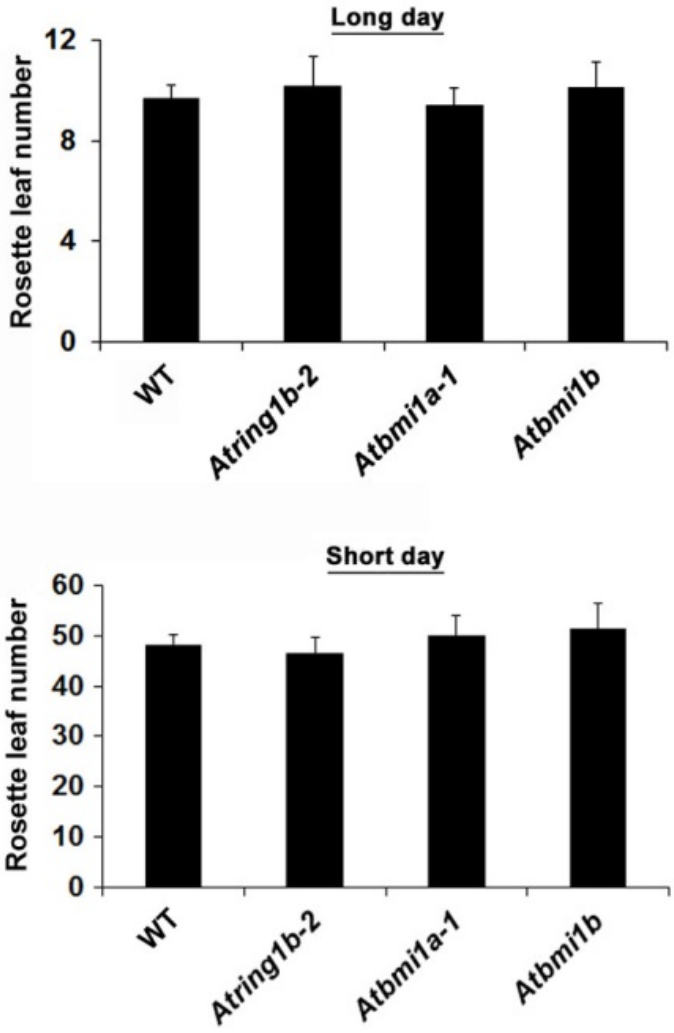

Fig. S1. ***Atring1b-2***, ***Atbmi1a-1*** **and** ***Atbmi1b*** **exhibit similar flowering time to wild-type plants under long days and short days.** Values were scored from at least 15 plants of each genotype. Error bars indicate s.d.

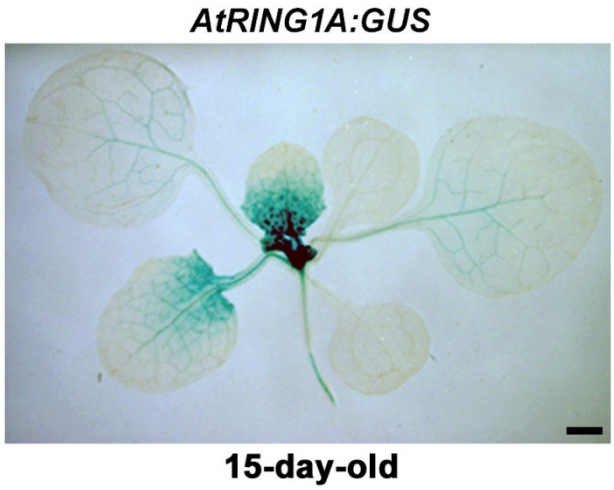

Fig. S2. GUS staining of a 15-day-old *AtRING1A:GUS* seedling. Bar = 1 mm.

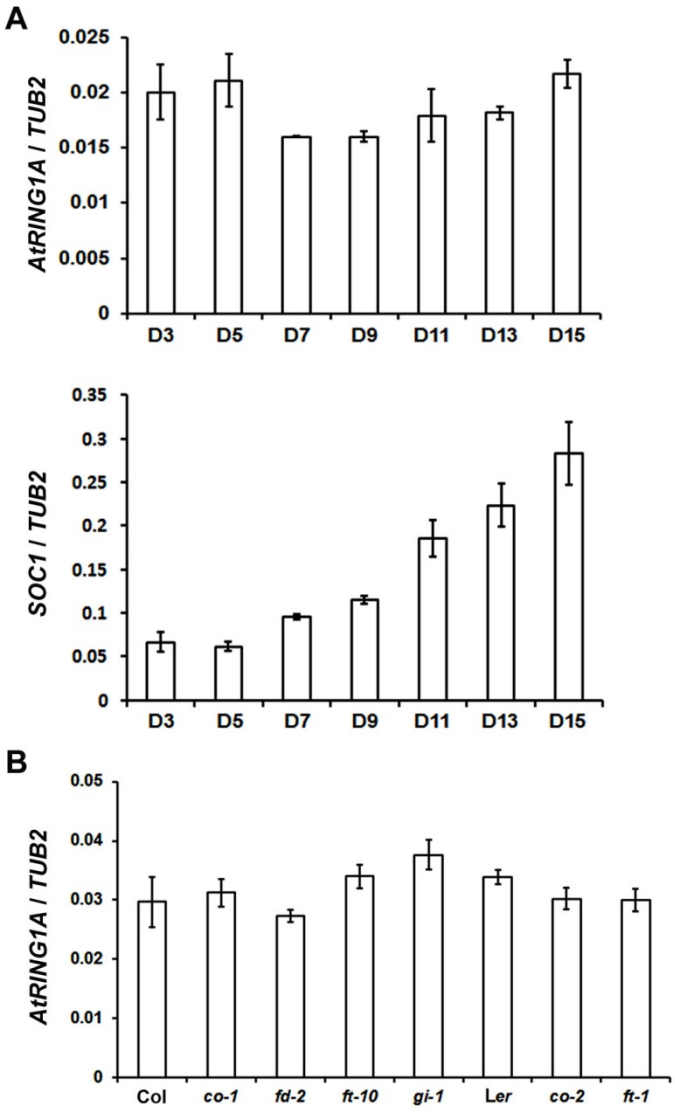

Fig. S3. *AtRING1A* expression is not affected by the photoperiod pathway. (**A**) Temporal expression of *AtRING1A* determined by quantitative real-time PCR in wild-type seedlings grown under LDs (upper panel). The expression of *SOC1*, which is regulated by the photoperiod pathway, was examined as a positive control (lower panel). Error bars indicate s.d. (**B**) *AtRING1A* expression determined by quantitative real-time PCR in 9-day-old mutants of the photoperiod pathway. *AtRING1A* expression was normalized to *TUB2* expression. Error bars indicate s.d.

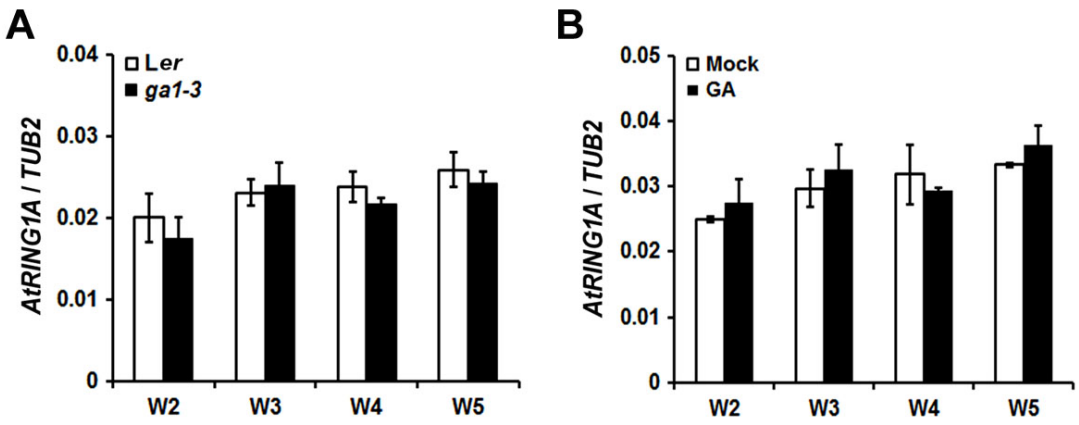

Fig. S4. *AtRING1A* expression is not affected by the GA pathway. (**A**) Comparison of *AtRING1A* expression in GA-deficient mutant *ga1-3* and wild-type plants. Seedlings grown under SDs from week 2 (W2) to week 5 (W5) were collected for expression analysis. Error bars indicate s.d. (**B**) Effect of GA treatment on *AtRING1A* expression in wild-type plants grown under SDs. Exogenous GA (100 μM) or 0.1% ethanol (mock) was applied weekly onto wild-type Col plants grown under SDs. Seedlings treated from week 2 (W2) to week 5 (W5) were collected for expression analysis. *AtRING1A* expression was normalized to *TUB2* expression. Error bars indicate s.d.

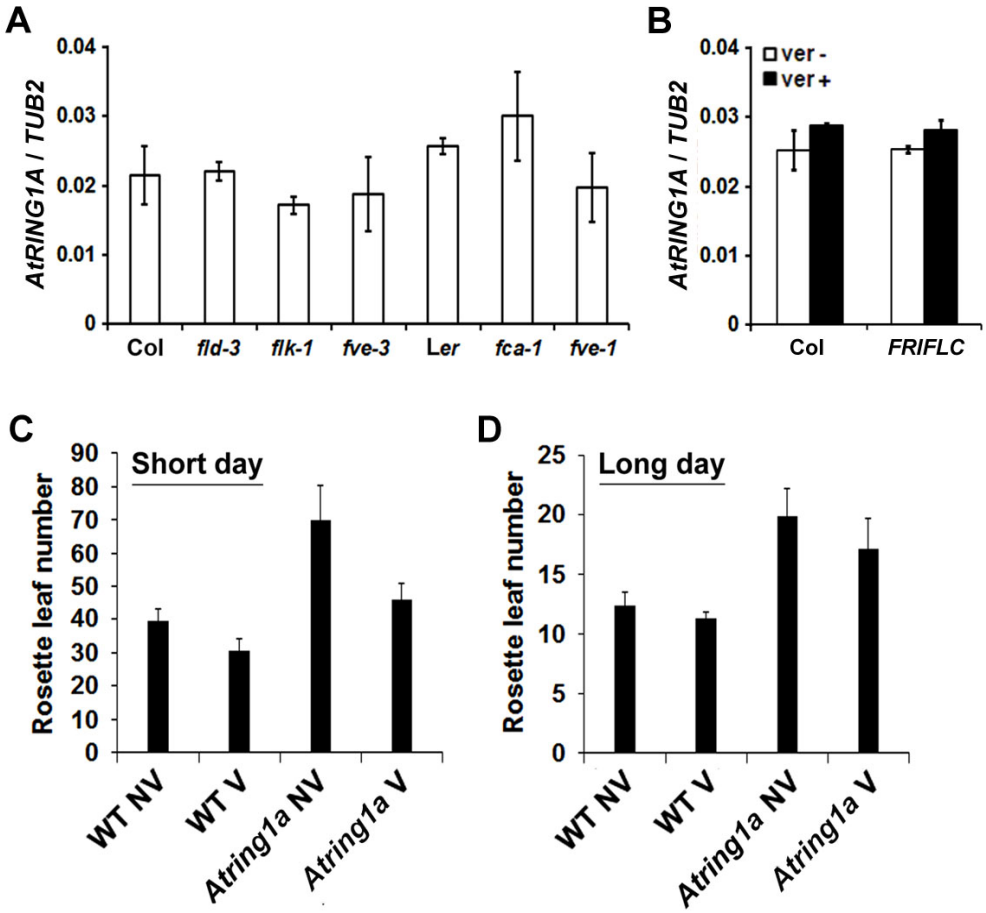

Fig. S5. *AtRING1A* expression is not regulated by the autonomous and vernalization pathways. (**A**) *AtRING1A* expression in 9-day-old mutants of the autonomous pathway grown under LDs. (**B**) Effect of vernalization treatment on *AtRING1A* expression. For vernalization treatment, seeds were sow on MS medium and vernalized at 4°C under low light condition for 8 weeks. The 9-day-old seedlings grown under LDs were harvested for expression analysis. *AtRING1A* expression in (**A**) and (**B**) was examined by quantitative real-time PCR, and normalized to *TUB2* expression. Error bars indicate s.d. (**C,D**) Flowering time of *Atring1a* and wild-type plants with (V) and without (NV) vernalization treatment grown under SDs (**C**) and LDs (**D**). After vernalization treatment, the seedlings were transferred to soil and grown under SDs or LDs. Values were scored from at least 15 plants of each genotype. Error bars indicate s.d.

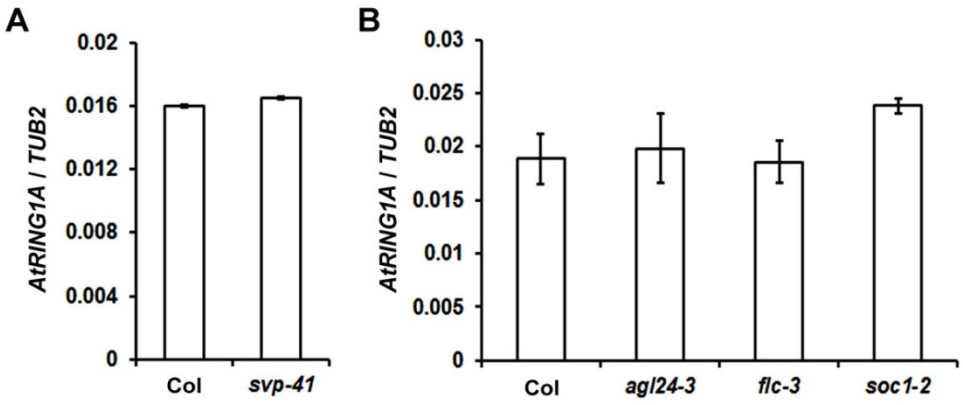

Fig. S6. *SVP*, *AGL24*, *SOC1* and *FLC* do not affect *AtRING1A* expression. (**A,B**) *AtRING1A* expression in several flowering time mutants. *AtRING1A* expression was examined by quantitative real-time PCR in 7-day-old wild-type and *svp-41* seedlings (**A**), and 9-day-old wild-type and several other mutant seedlings (**B**) grown under LDs. *AtRING1A* expression was normalized to *TUB2* expression. Error bars indicate s.d.

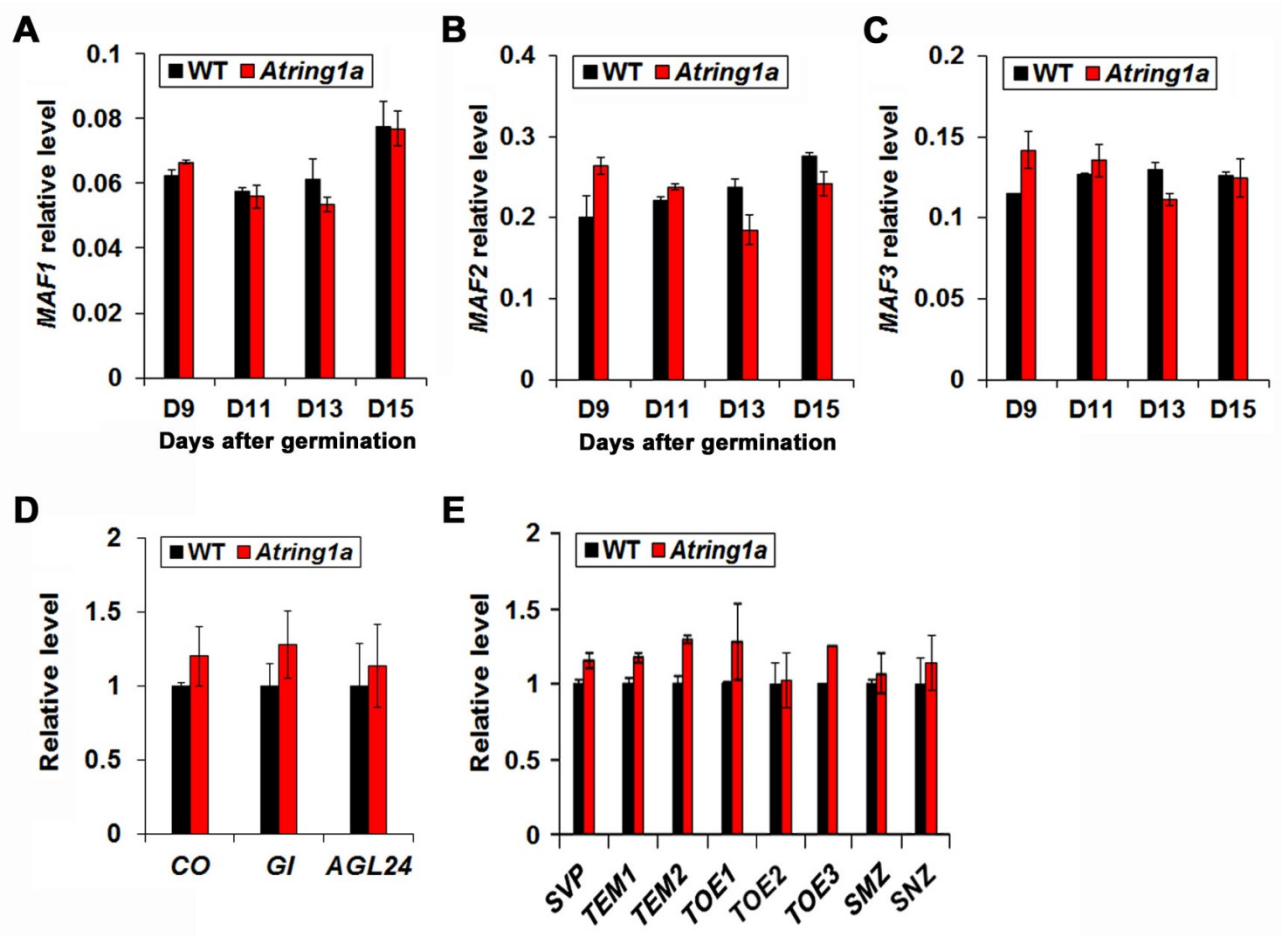

Fig. S7. Expression of *MAF1*, *MAF2*, *MAF3*, and other important floral repressors is not regulated by *AtRING1A*. (**A-C**) Temporal expression of *MAF1* (**A**), *MAF2* (**B**) and *MAF3* (**C**) determined by quantitative real-time PCR in developing *Atring1a* and wild-type seedlings grown under LDs. Gene expression was normalized to *TUB2* expression. (**D**,**E**) Expression of *CO*, *GI* and *AGL24* (**D**), and *SVP*, *TEM1*, *TEM2*, *TOE1*, *TOE2*, *TOE3*, *SMZ* and *SNZ* (**E**) determined by real-time PCR in 9-day-old *Atring1a* and wild-type seedlings grown under LDs. Gene expression was normalized to *TUB2* expression, and expression levels in wild-type seedlings are all set as 1. Error bars indicate s.d.

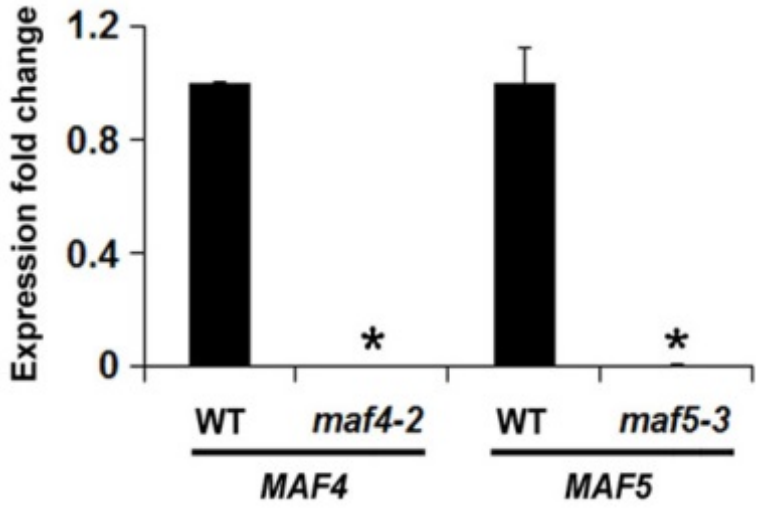

Fig. S8. Expression of *MAF4* and *MAF5* is undetectable in *maf4-2* and *maf5-3*, respectively. Gene expression was determined by quantitative real-time PCR in 9-day-old wild-type and mutant plants. Results were normalized against the expression levels of *TUB2*. Asterisks indicate that quantitative real-time PCR analysis of *MAF4* and *MAF5* in *maf4-2* and *maf5-3* obtains very high Ct values, respectively, because of their barely detectable levels.

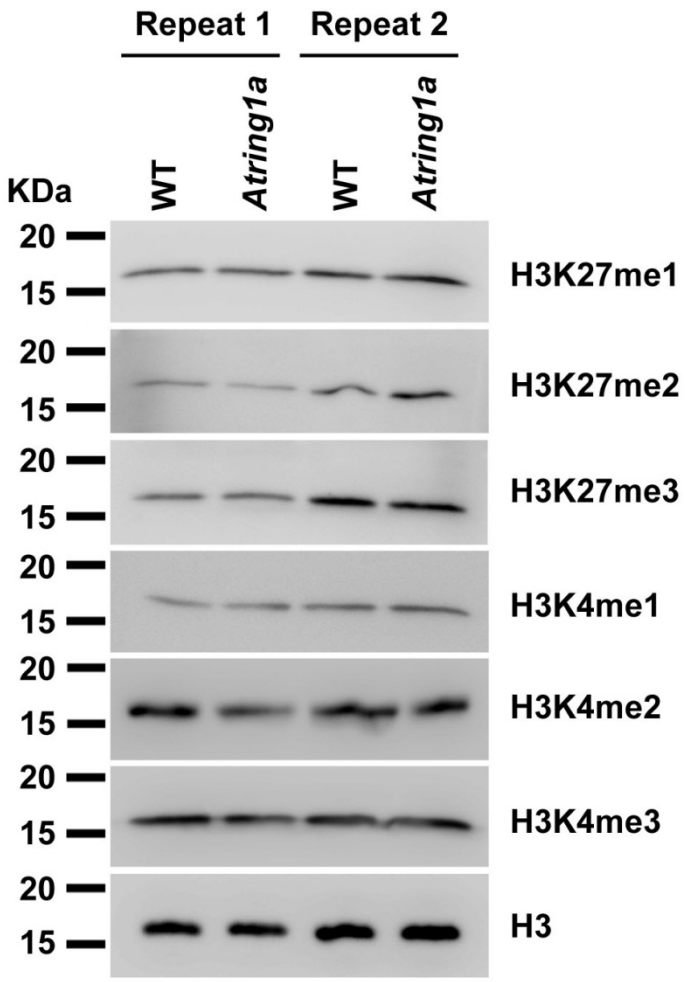

Fig. S9. Analysis of global H3K27 and H3K4 methylation levels in wild-type and *Atring1a* plants by immunoblotting. Nuclear extracts of 9-day-old *Atring1a* and wild-type seedlings were subjected to Western blot analysis using various antibodies.

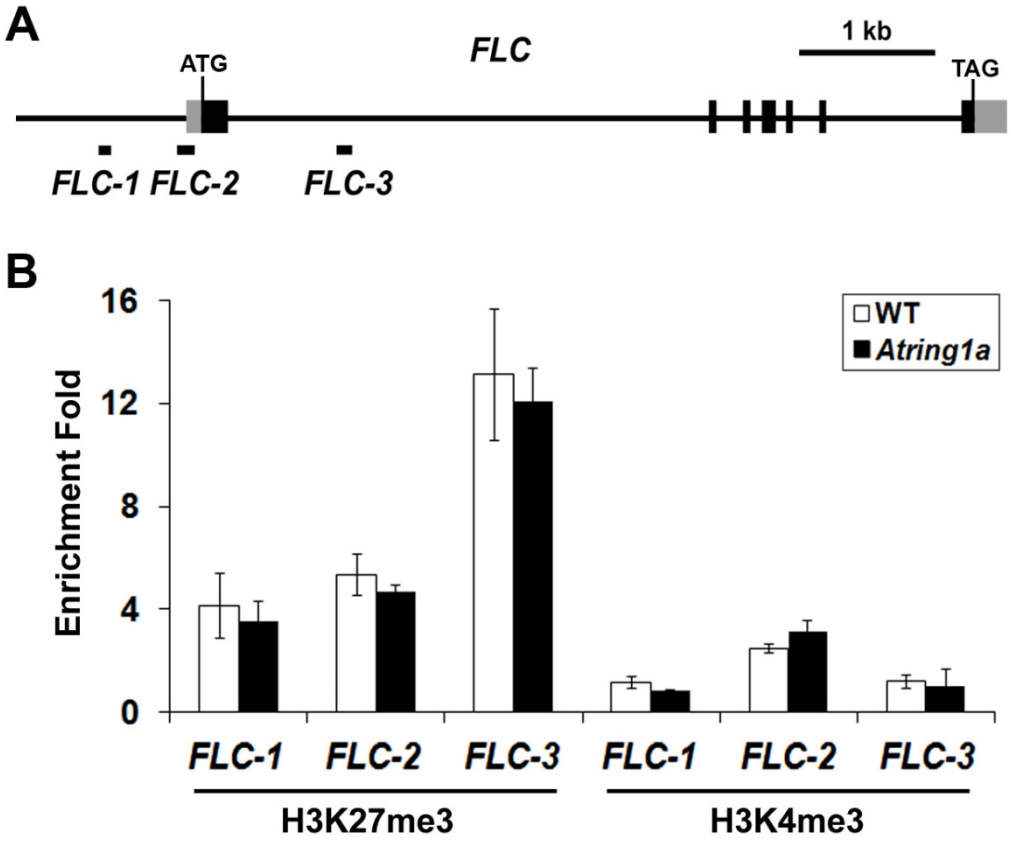

Fig. S10. *AtRING1A* does not obviously affect H3K27me3 and H3K4me3 enrichment at *FLC*. (**A**) Schematic diagram of the *FLC* genomic region. Exons and untranslated regions are represented by black and grey boxes, respectively, while introns and other genomic regions are represented by black lines. The translation start site (ATG) and stop codon (TAG) are indicated. DNA fragments amplified in ChIP assays are indicated below the *FLC* genomic region that carries both H3K27me3 and H3K4me3 marks. (**B**) ChIP analysis of H3K27me3 and H3K4me3 levels at *FLC* in 9-day-old wild-type and *Atring1a* seedlings. Error bars indicate s.d. of three biological replicates.

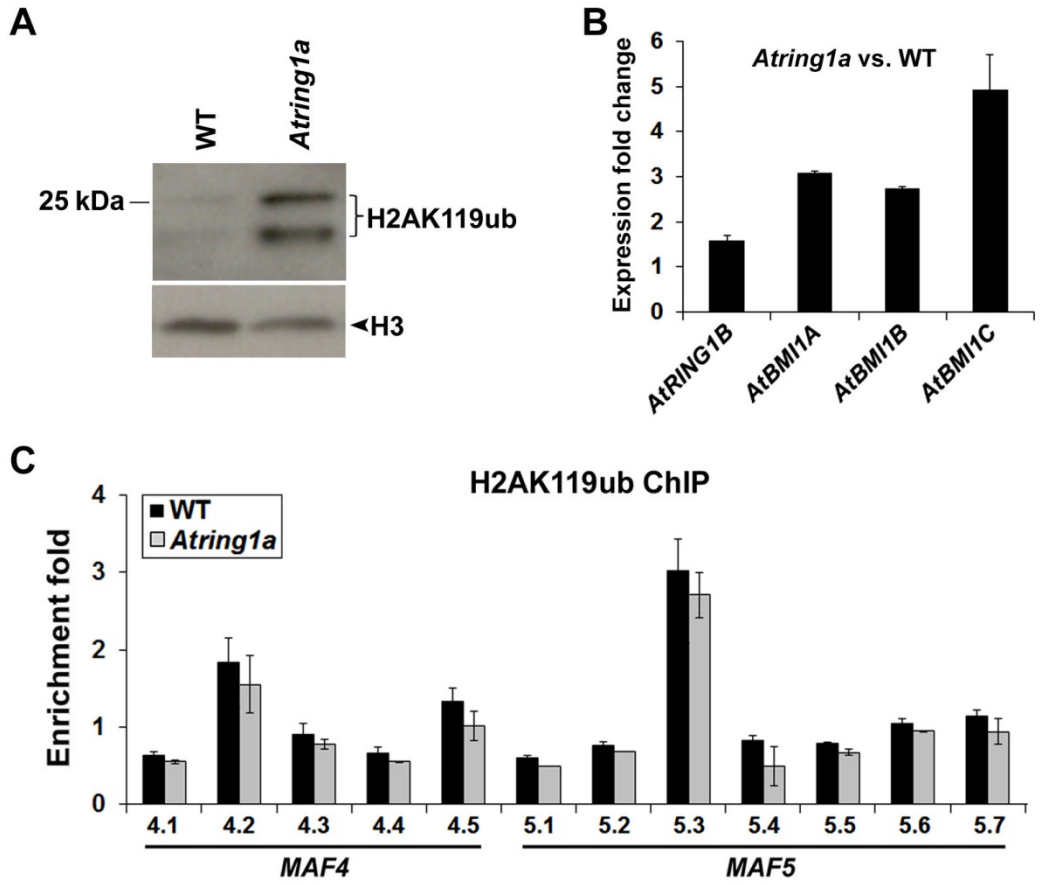

Fig. S11. *AtRING1A* does not significantly affect H2AK119ub levels at *MAF4* and *MAF5*. (A) Analysis of global H2AK119ub levels in wild-type and *Atring1a* plants by immunoblotting. Nuclear extracts of 9-day-old *Atring1a* and wild-type seedlings were subjected to Western blot analysis using anti-H2AK119ub and anti-H3 antibodies**.** The different bands shown in the blot indicate different H2Aub isoforms. **(B)** Quantitative real-time PCR analysis of expression of *AtRING1B*, *AtBMI1A*, *AtBMI1B* and *AtBMI1C* in 9-day-old *Atring1a* and wild-type seedlings grown under LDs. Results were normalized against the expression levels of *TUB2*. Gene expression levels in wild-type seedlings are all set as 1. **(C)** ChIP analysis of H2AK119ub levels at *MAF4* and *MAF5* in 9-day-old wild-type and *Atring1a* seedlings. A genomic fragment of *ACTIN7* (*At5g09810*) was amplified as an internal control for measurement of H2AK119ub enrichment. Error bars indicate s.d of three biological replicates. There is no statistically significant difference in ChIP enrichment fold between wild-type and *Atring1a*.

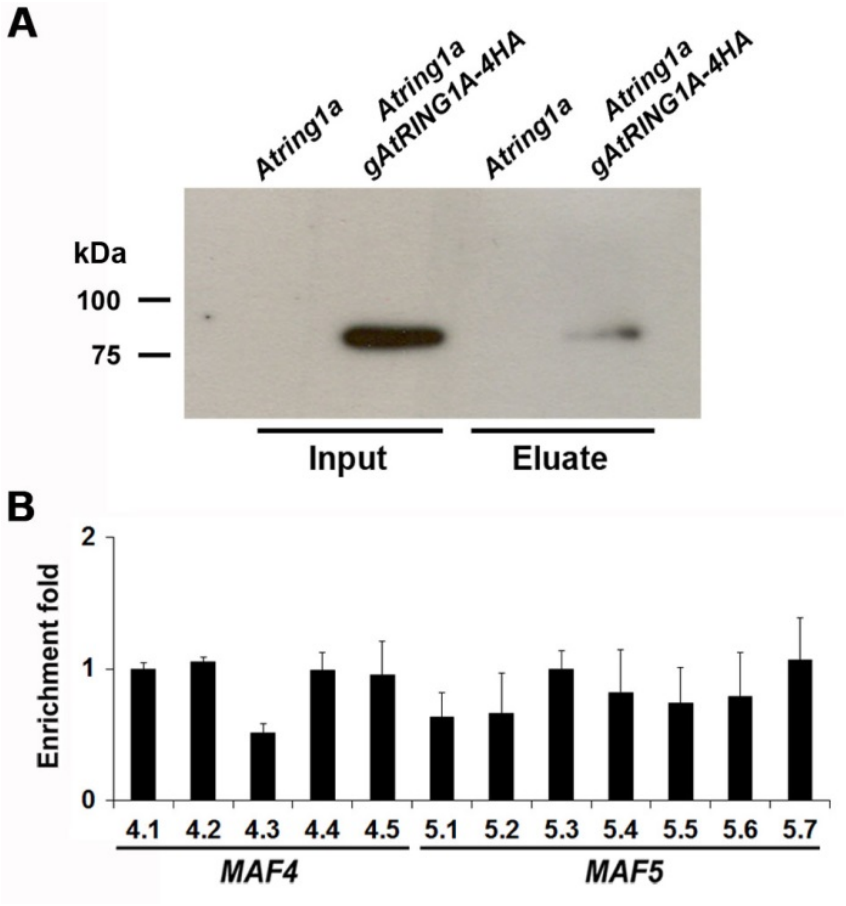

Fig. S12. AtRING1A is not associated directly with *MAF4* and *MAF5* genomic regions. (**A**) Western blot analysis using anti-HA antibody shows the expression of AtRING1A-4HA in nuclear extracts (Input) or immunoprecipitated fractions (Eluate) of 9-day-old *Atring1a gAtRING1A-4HA* seedlings. (**B**) ChIP analysis shows no significant binding of AtRING1A-4HA to *MAF4* and *MAF5* genomic regions. Enrichment fold was calculated first by normalizing the amount of a target DNA fragment against a genomic fragment of *ACTIN7*, and then by normalizing the value for *Atring1a gAtRING1A-4HA* against that for *Atring1a*. Error bars indicate s.d. of three biological replicates.

Table S1. Primers used in this study

Primers pairs used for plasmid construction

Primer name	Primers
gAtRING1A-F	5′-CACCTAACTCAGCAGGACAAGGAGG-3′
gAtRING1A-R	5′-CTGTTAAAAAGTAAAAAAGACTAAGC-3′
gAtRING1A-4HA-F	5′-ACCGGAAGAAGCAAACTGAGTATCCATATGACGTTCCAGA-3′
gAtRING1A-4HA-R	5′-TTAGGCTCCAAGTTTCTTCATCTAGTAGCGTAATCTGGAA-3′
gAtRING1A-F (EcoRI)	5′-CGGAATTCTAACTCAGCAGGACAAGGAGG-3′
gAtRING1A-R (BamHI)	5′-CGGGATCCCTCAGTTTGCTTCTTCCGGTA-3′

Primers pairs used for gene expression analysis (quantitative real-time PCR)

Gene name	Primers
SOC1	5′-AGCTGCAGAAAACGAGAAGCTCTCTG-3′ 5′-GGGCTACTCTCTTCATCACCTCTTCC-3′
FT	5′-CTTGGCAGGCAAACAGTGTATGCAC-3′ 5′-GCCACTCTCCCTCTGACAATTGTAGA-3′
FLC	5′-CTAGCCAGATGGAGAATAATCATCATG-3′ 5′-TTAAGGTGGCTAATTAAGTAGTGGGAG-3′
SVP	5′-CAAGGACTTGACATTGAAGAGCTTCA-3′ 5′-CTGATCTCACTCATAATCTTGTCAC-3′
AGL24	5′-GAGGCTTTGGAGACAGAGTCGGTGA-3′ 5′-AGATGGAAGCCCAAGCTTCAGGGAA-3′
CO	5′-TCAGGGACTCACTACAACGACAATGG-3′ 5′-TTGGGTGTGAAGCTGTTGTGACACAT-3′
GI	5′-GGGTAAATATGCTGCTGGAGA-3′ 5′-CAGTATGACACCAGCTCCATT-3′
MAF1	5′-GGCATAACCCTTATCGGAGATTTGAAGCCA-3′ 5′-CTTTGTCGATGAGACCATTGCGTCGTTTG-3′
MAF2	5′-AACTCGGAATTATCTGCCACTCAAAG-3′ 5′-CTTCCCCCATCATTAGTTCTGTCTTC-3′

MAF3	5′-GAAAGGGAGAAGTTGCTGATAGAAGAG-3′ 5′-AGCACAAGAACTCTGATATTTGTCTAC-3′
MAF4	5′-TGGCCAAGATCCTCAGTCGTTATGA-3′ 5′-GCTGCTCTTCCAGGGACTTTAGACA-3′
MAF5	5′-GATGGAGCTTGTGAAGAACCTTCAGG-3′ 5′-CAGCCGTTGATGATTGGTGGTTACTTG-3′
TEM1	5′-ATCCACTGGAAAGTCCGGTCTA-3′ 5′-GAATAGCCTAACCACAGTCTGAACC-3′
TEM2	5′-TGGTCCGAGAGAAAACCCG-3′ 5′-TCAACTCCGAAAAGCCGAAC-3′
TOE1	5′-CAGCGTGGAGTTAGCTTGAGG-3′ 5′-CGTTCCAGTAAAGGCGATGATCC-3′
TOE2	5′-ATGGAGAACCACATGGCTGC-3′ 5′-GGTGCTGTAGCTGCTACGGC-3′
TOE3	5′-GATCTTAGCTCAGAGACGACGAG-3′ 5′-CATTGCTAGCGATAGATCGCTC-3′
SMZ	5′-AGGGAGAAGGAGCCATGAAGTTTGGTG-3′ 5′-GTCTTCAGAGGTTTCATGGTTGCCATG-3′
SNZ	5′-CAGCAGATTATTACATGGGTTTG-3′ 5′-GGTTTAATTTCTGTGATCGGTAGA-3′
AtRING1A	5′-ATCTCTGTTGCCGACCCACT-3′ 5′-GCCGCATCTTCTCCTACTCT-3′
TUB2	5′-ATCCGTGAAGAGTACCCAGAT-3′ 5′-AAGAACCATGCACTCATCAGC-3′

Primers pairs used for gene expression analysis (semi-quantitative PCR)	
Gene name	**Primers**
AtRING1A	5′-CCATCTTCTATATCTGGAGACC-3′ 5′-GTGTTGAACGACTTGTAGACCG-3′
TUB2	5′-ATCCGTGAAGAGTACCCAGAT-3′ 5′-TCACCTTCTTCATCCGCAGTT-3′

Primers pairs used for ChIP assays (quantitative real-time PCR)	
Product name	**Primers**
FLC-1	5′-CAAGCTGATACAAGCATTTCACCAA-3′ 5′-TTGAGCTATTGCCATATGTGTGGACA-3′

FLC-2	5′-CCGACGAAGAAAAAGTAGATAGGCAC-3′ 5′-CCCAAACCTGAGGATCAAATTAGG-3′
FLC-3	5′-CTTTGAATCACAATCGTCGTGTG-3′ 5′-ACGTGCATATACAAATCCAAGAGAAC-3′
MAF3 (3.1)	5′-GTCTAGCCCAAAAGAAGAAGATAGAAACG-3′ 5′-GGAGGCAGAGTCGTAGAGTTTTCC-3′
MAF4 (4.1)	5′-CCATAATTTAAATATGGTGGCCCA-3′ 5′-AGCCGAACCAAATTTCAAACC-3′
MAF4 (4.2)	5′-CGGCGAGTTATGCAGACATCACA-3′ 5′-GTGGCAGAGATGATGATAAGAGCGA-3′
MAF4 (4.3)	5′-AGGGTCTATAGACTGGAACAGATGC-3′ 5′-GCTAGCTAGAACCCTTTTCCTTAAGC-3′
MAF4 (4.4)	5′-GCTAGTTTCTTGGTAGCTCGGCTG-3′ 5′-CATTCTTACTTCGTGTCGTCTGTGATC-3′
MAF4 (4.5)	5′-ATTCTTGAATCCTCTGAAACTCCG-3′ 5′-TGGACACCATCACAACTTTATTCAG-3′
MAF5 (5.1)	5′-TACTGTTAAGCCCAGATTCGGC-3′ 5′-ATTGATGTCAATCGCGTACCCT-3′
MAF5 (5.2)	5′-GTTTCTCATACAGCCCAATACATGC-3′ 5′-GATTGGATTTAGTTCATTCCACCG-3′
MAF5 (5.3)	5′-CAGGATCTCCGACCAGTTTATACAGAC-3′ 5′-GAGGAGTTGTAGAGTTTGCCGGT-3′
MAF5 (5.4)	5′-CGTGGTGGTAATCCGTAATTCATGT-3′ 5′-CAAATGGCACTCGTTTCCACTAGA-3′
MAF5 (5.5)	5′-GTGTTTTCGCTTGAGATTGTGGT-3′ 5′-CGTGATGTCCGTGATCTATTGC-3′
MAF5 (5.6)	5′-GAAAGAGAAAATTGTGTCCTGGAAA-3′ 5′-CTCTATTGAATTGTTAGTTGTTCCGC-3′
MAF5 (5.7)	5′-CTACACACTTTCTGGTGAAACCC-3′ 5′-CAGTTCTTAAAATGATCTTTTCATGTG-3′
TUB2	5′-ATCCGTGAAGAGTACCCAGAT-3′ 5′-AAGAACCATGCACTCATCAGC-3′
ACT7	5′-CGTTTCGCTTTCCTTAGTGTTAGCT-3′ 5′-AGCGAACGGATCTAGAGACTCACCTTG-3′

MU	5′-TTACAAGGAATCTGTTGGTGGT-3′ 5′-AACATAGGTTTAGAGCATCTGC-3′	